Performance Analysis and Optimization of Tc-DTR IR-UWB Receivers over Multipath Fading Channels with Tone Interference

Marco Di Renzo, Dario de Leonardis, Fabio Graziosi, Fortunato Santucci

Performance Analysis and Optimization of $\mathrm{T_C}$–DTR IR–UWB Receivers over Multipath Fading Channels with Tone Interference

Marco Di Renzo, *Member, IEEE*, Dario De Leonardis, Fabio Graziosi, *Member, IEEE*, and Fortunato Santucci, *Senior Member, IEEE*

***Abstract*— In this paper, we analyze the performance of a particular class of Transmitted–Reference (TR) receivers for Impulse Radio (IR–) Ultra Wide Band (UWB) communication systems, which is called Chip–Time Differential Transmitted–Reference ($\mathrm{T_c}$–DTR). The analysis aims at investigating the robustness of this receiver to single– and multi–tone Narrow–Band Interference (NBI), and at comparing its performance with other non–coherent receivers proposed in the literature. It is shown that the $\mathrm{T_c}$–DTR scheme provides more degrees of freedom for performance optimization, and it is inherently more robust to NBI than other non–coherent receivers. More specifically, it is analytically proved that the performance improvement is due to the chip–time level differential encoding/decoding of the Direct Sequence (DS) code, and to an adequate design of DS code and average pulse repetition time. The analysis encompasses performance metrics that are useful for both data detection (*i.e.*, Average Bit Error Probability, ABEP) and timing acquisition (*i.e.*, False Alarm Probability, $\mathrm{P_{fa}}$, and Detection Probability, $\mathrm{P_d}$). Moving from the proposed semi–analytical framework, the optimal code design and system parameters are derived, and it is highlighted that the same optimization criterion can be applied to all performance metrics considered in this paper. Also, analytical frameworks and theoretical findings are substantiated via Monte Carlo simulations.**

***Index Terms*— Ultra wide band (UWB), impulse radio (IR), transmitted–reference (TR), tone interference, multipath fading channels, code design, performance analysis.**

I. Introduction

TRANSMITTED–REFERENCE (TR) signaling schemes in conjunction with auto–correlation receiver architectures are well–known techniques to transmit and receive data over unknown fading channels (see, *e.g.*, [1], [2]). These receiver schemes are today experiencing a renewed and increasing interest for their application to the design of low–complexity Impulse Radio (IR–) Ultra Wide Band (UWB) communication systems [3]–[5]. The interested reader is referred to [6] for a recent comprehensive overview. As a matter of fact, TR receivers can exploit the inherent multipath diversity capability offered by the large transmission bandwidth of IR–UWB signals without the need of either complicated channel estimation techniques or stringent timing acquisition requirements. Moreover, frequency–dependent effects of the UWB channel are straightforwardly taken into account by TR schemes. These properties are particulary suited for a low–complexity receiver design and operation in those application scenarios where conventional/optimal receiver architectures, *e.g.*, Rake schemes [7], might result in a too complicated system design [8]. However, the claimed low–complexity receiver design of TR schemes for channel estimation and timing synchronization operations is sometimes shadowed by the need of wide–band analog delay lines, which might be tens of nanoseconds long for typical UWB channels [8]–[10]. Although this might not be a fundamental problem for realizing proof–of–concept prototypes, this is certainly an important issue to be considered for an integrated receiver design [11], [12]. Due to these reasons, recent research efforts on the design of UWB receivers have focused on the application of the Compressive Sampling (CS) approach, which promises to solve some of the inherent difficulties of coherent (full–digital) and non–coherent (based on analog delay lines) UWB receivers. The interested reader might consult [13]–[17] for further information. In this paper, regardless of the practical implementation used to acquire the UWB signal at the receiver end, our main goal is to study, from the theoretical point of view, the performance of TR–UWB receivers in the presence of single– and multi–tone interference, and compare various receiver proposals available in the literature. To our best knowledge, such a comprehensive performance study is still unavailable in the literature.

Moving from the first proposal of application to IR–UWB communication systems [3], several non–coherent receiver schemes are today available in the open technical literature (see, *e.g.*, [11]–[35] and references therein), as well as many studies have been conducted to figure out their achievable performance over realistic propagation environments (see, *e.g.*, [36]–[50] and references therein). In particular, in [18] the concept of detection and timing using dirty templates has

Manuscript received November 8, 2010; revised April 23, 2011. First published XXX XXX, XXX; current version published XXX XXX, XXX. This paper was presented in part at the IEEE International Conference on Ultra–Wideband (ICUWB), Vancouver, Canada, Sep. 2009; and at the IEEE Military Communications Conference (MILCOM), Boston, MA, Oct. 2009. The review of this paper was coordinated by Prof. Robert Qiu.

M. Di Renzo is with L2S, UMR 8506 CNRS – SUPELEC – Univ Paris–Sud, 3 rue Joliot–Curie, 91192 Gif–sur–Yvette CEDEX (Paris), France, (e–mail: marco.direnzo@lss.supelec.fr).

D. De Leonardis, F. Graziosi, and F. Santucci are with the Department of Electrical and Information Engineering and the Center of Excellence for Research DEWS, University of L'Aquila, Via G. Gronchi, 18, 67100 L'Aquila, Italy, (e–mail: {fabio.graziosi, fortunato.santucci}@univaq.it).

Color versions of one or more of the figures in this paper are available online at http://ieeexplore.ieee.org.

Digital Object Identifier XXX.XXX/TVT.XXX.XXX

been introduced; in [22] a hybrid detection method composed by a matched filter followed by an auto–correlation receiver has been considered for performance improvement; in [11] a Slightly Frequency–Shifted Reference (FSR) receiver has been introduced to avoid analog delay lines that afflict the efficient design at the IC–level of conventional TR methods; in [29] a Differential TR (DTR) scheme with chip–time processing has been designed and its performance analyzed; in [30] a pulse cluster transmission system has been conceived to reduce the length of the analog delay line and make its implementation affordable; in [12] the authors have moved from [3] and [11] to present a receiver scheme that avoids delay lines and transmits the reference signal over an orthogonal code; in [33], the scheme in [12] is further extended to the reference scenario with multiple–access interference and its design flexibility is studied. Moreover, analytical studies in [37], [38] have allowed us to fully understand the performance of TR receiver schemes over multipath fading channels further impaired by single–tone Narrow–Band Interference (NBI). These studies have been extended in [42], [49] for detection and synchronization analysis, and in [41], [44], [45] to analyze the performance of Energy Detector (ED) receivers impaired by aggregate NBI interference. In [50], the effect of uncoordinated UWB (and, so, wide–band) interference on the performance of ED receivers has been recently studied as well. Furthermore, in [46] an advanced framework has been proposed to avoid some limitations evidenced in [37] to account for different front–end zonal filters at the receiver input. Finally, in [48] the performance of TR systems for application to relay networks has been investigated.

While first investigations on the performance analysis, design and optimization of IR–UWB coherent and non–coherent receiver schemes have been mainly devoted to the multipath fading scenario, with the main aim to quantify the energy collection capabilities of them in harsh propagation environments, recently the interest has moved towards coexistence issues in the presence of NBI (see, *e.g.*, [51]–[59] and references therein, along with [60], [61] for a survey, recent results, and a comprehensive reference list). As a matter of fact, if on the one hand the large transmission bandwidth of IR–UWB signals allows them to resolve multipath components and exploit multipath diversity, thus making this technology a viable candidate for communications in harsh reference scenarios, such as industrial/factory indoor and forest/sub-urban outdoor environments, on the other hand it yields some new design challenges from the point of view of coexistence: the successful deployment of IR–UWB systems requires that they coexist and contend with a variety of interfering signals. For example: i) unlicensed commercial UWB–based systems are currently envisioned to operate with low power spectral density levels over already–populated frequency bands, an operating scenario that is receiving even more attention today under the broader umbrella of underlay Cognitive Radio (CR) [59], and ii) intentional jammers are inevitably present in many military contexts [62], and IR–UWB systems must be robust against jamming.

As far as TR or non–coherent receiver schemes are considered, the problem of coexistence is even exacerbated due to the incoherent processing. Performance studies in [38], [41]–[44] have clearly shown that the error probability of these receivers gets significantly worse in the presence of interference, and have also pointed out that the performance gain offered by a receiver in a multipath environment might disappear in the presence of interference [41]. These results have been the driver for significant research efforts to develop robust interference cancelation mechanisms to improve the overall performance and coexistence capabilities of non–coherent solutions (see, *e.g.*, [40], [43], [63]–[67] and references therein).

Motivated by the above considerations, the aim of this paper is twofold: i) to assess the performance of the recently proposed Chip–Time Differential Transmitted–Reference ($\mathrm{T_c}$–DTR) receiver scheme [29] in a reference scenario with multipath fading and tone interference, and ii) to compare its performance and design flexibility with some other notable TR schemes. Our analysis shows that the particular structure of the $\mathrm{T_c}$–DTR scheme, which uses Direct Sequence (DS) coding and a processing at the chip–time ($\mathrm{T_c}$) level, allows it to reject tone interference via a simple design of the DS code, in addition to the optimization of some system parameters, *e.g.*, the chip–time and the shape of the transmitted pulse. Guidelines for the design of the optimal code are derived, and it is pointed out that, for moderately low Signal–to–Interference Ratios (SIRs), tone interference can be almost completely canceled out. The analysis encompasses performance metrics that are useful for both data detection (*i.e.*, Average Bit Error Probability, ABEP) and timing acquisition (*i.e.*, False Alarm Probability, $\mathrm{P_{fa}}$, and Detection Probability, $\mathrm{P_d}$), and it is pointed out that, among the analyzed receivers, the $\mathrm{T_c}$–DTR scheme provides the best performance and design flexibility. Reference scenarios with single– and multi–tone NBI are studied, and unlike recent papers (see, *e.g.*, [41], [50]), we consider the case–study where multiple jammers can transmit at different carrier frequencies. We show that NBI can be rejected *deterministically* if a single jammer falls within the transmission bandwidth of the UWB signal, while it can be rejected only *statistically*, *i.e.*, on average, if multiple jammers are simultaneously transmitting at different frequencies. Although single– and multi–tone interference modeling might appear very simplified models, they have been extensively used in the literature due to their analytical simplicity to get fundamental insightful information about the performance of complicated receiver structures (see, *e.g.*, [37], [38], [41], [42], [44], [50], [60], and [53] for some comments about their validity). In this paper, we consider these two models for the jamming signals for two reasons: i) the analytical simplicity, and thus the possibility to get simple and insightful closed–form expressions, and ii) the widespread adoption of these models, which allow us to compare our analysis with other studies available in the literature, thus having a common basis for performance comparison of various TR schemes [45]. Furthermore, analytical results are substantiated via numerical simulations, and performance comparison with other non–coherent receivers is provided as well.

The remainder of this paper is organized as follows. Section II introduces the system model and the $\mathrm{T_c}$–DTR receiver. In Section III, the framework for performance analysis over

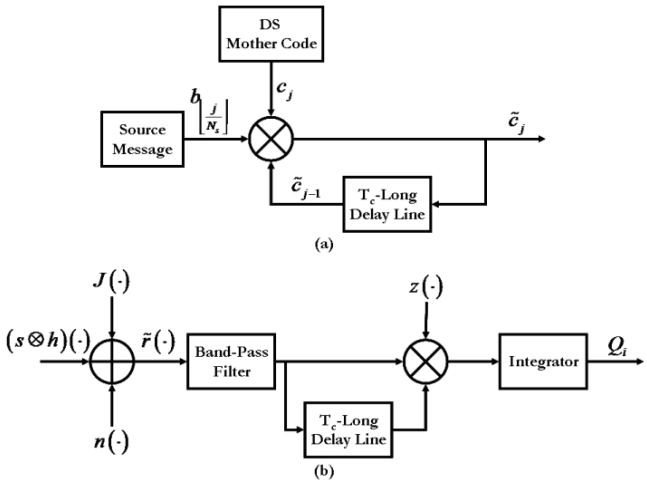

Fig. 1. Block diagram of the $\mathrm{T_c}$–DTR scheme: (a) transmitter, (b) receiver.

frequency–selective multipath channels and a faded single–tone NBI is presented. Section IV extends the latter framework to the scenario with multiple jammers, and provides comments about its accuracy and limitations. In Section V, the optimal DS code and system design for NBI suppression are derived, and in Section VI the robustness of the $\mathrm{T_c}$–DTR receiver is compared to other non–coherent TR solutions. In Section VII, some numerical results are shown to substantiate claims and analytical findings. Finally, Section VIII concludes the paper.

II. System Model

Let us consider the $\mathrm{T_c}$–DTR receiver scheme shown in Fig. 1. With respect to conventional TR solutions (see, *e.g.*, [37], [38], [41]) that resort to Time–Hopping (TH) spreading mechanisms, the proposed solution uses DS coding, in which the transmitted signal is given, for every signaling interval, by a sequence of N_s short UWB pulses, whose polarity depends on the DS code. The reader may find in [29] further information about the rationale of using DS instead of TH solutions for DTR receivers. In this paper, we are mainly interested in showing that using DS instead of TH coding can be beneficial, for both data detection and timing acquisition, to reject tone interference via a proper code design.

A. Transmitted Signal

1) Data Detection: As far as data detection is concerned, we assume a Binary Pulse Amplitude Modulation (BPAM) scheme to convey the information bits. Accordingly, the signal transmitted by a generic user can be written as follows:

$$s(t) = \sum_{j=-\infty}^{+\infty} \sqrt{E_w} \tilde{c}_j w\left(t - jT_c - \left\lfloor \frac{j}{N_s} \right\rfloor T_b\right) \qquad (1)$$

where $\{b_i\}_{i=-\infty}^{+\infty} \in \{-1,+1\}$ is the i–th transmitted information bit, $\{c_j\}_{j=0}^{N_s-1} \in \{-1,+1\}$ is the signature DS code with period N_s, *i.e.*, $\{c_j\}_{j=0}^{N_s-1} = \{c_{j+N_s}\}_{j=0}^{N_s-1}$, $\tilde{c}_j = \left(b_{\lfloor j/N_s \rfloor} c_j\right) \tilde{c}_{j-1}$ is the jointly differentially–encoded version of b_i and c_j, and $\lfloor \cdot \rfloor$ is the lower integer part operator. Moreover, $T_b = N_s T_c$ is the bit duration with T_c denoting the average pulse repetition period, *i.e.*, the chip–time, $w(\cdot)$ is the band–pass[1] transmitted pulse with duration T_w, center frequency f_c, and unit energy (*i.e.*, $\int_0^{T_w} w^2(t)\,dt = 1$), $E_w = E_b/N_s$ and E_b are pulse and bit energies, respectively, and $\mathrm{DF} = T_w/T_c$ is the DS Duty Factor, which is representative of the impulsiveness of IR–UWB signaling. More specifically, (1) shows that the proposed $\mathrm{T_c}$–DTR receiver turns out to be a pulse–differential TR scheme in which the transmitted pulse train is weighted by a bipolar code, which is obtained by differentially encoding the information bits and a mother DS code.

Unlike typical TR schemes, which adopt TH coding instead of DS coding (see, *e.g.*, [37], [38], [41]), (1) clearly shows that the $\mathrm{T_c}$–DTR receiver completely avoids pulse dithering, which, as explained in detail in [29], can be beneficial to reduce the length of the delay line. However, the pulse dithering effect introduced by TH codes is often exploited to smooth the power spectrum of the transmitted signal and to comply with current regulations for UWB transmission. In spite of that, we wish to emphasize here that avoiding TH coding is not a limitation of the $\mathrm{T_c}$–DTR scheme since a similar spectrum smoothing effect can be obtained by properly designing the DS code in (1) (see, *e.g.*, [68] for further details). In other words, when taking into account all the requirements of IR–UWB transmissions, the DS code of the $\mathrm{T_c}$–DTR receiver should be optimized to meet multiple design criteria, which include, among the others, the rejection of NBI and the shaping of the power spectrum of the transmitted signal. Due to space constraints, in this paper we limit our attention to study the design of the DS code to reduce the effect of NBI and postpone the optimization of the DS code to meet multiple design requirements to a future research contribution.

2) Timing Acquisition: As far as timing acquisition is concerned, we assume a data–aided synchronization method that foresees the transmission of an unmodulated train of pulses before data transmission (see, *e.g.*, [29], [42], and [49] and references therein for a survey). Accordingly, the signal transmitted by a generic user can be written as follows:

$$s(t) = \sum_{j=-\infty}^{+\infty} \sqrt{E_w} \tilde{c}_j w(t - jT_c) \qquad (2)$$

where the same symbols and definitions as in (1) have been adopted. However, in this case E_b simply denotes the energy of each transmitted codeword (*i.e.*, a N_s–long train of pulses).

B. Channel Model

We consider a frequency–selective multipath fading propagation channel further impaired by NBI. The received signal,

[1]For the sake of clarity, we emphasize here that we adopt the terminology "band–pass pulse" to identify a pulse whose frequency power spectrum is not necessarily located around the zero frequency. The power spectrum can be centered around any frequency $f_c \gg 1$ in order to comply with current regulations for UWB transmission. However, no explicit frequency up–conversion is assumed in this paper, but the spectrum occupancy is determined only by the shape of the transmitted pulse. This is the main reason why the signal and channel models (see Section II-B) adopted in this manuscript are inherently real and are not complex.

$r(\cdot)$, can be written as follows:

$$r(t) = (s \otimes h)(t) + J(t) + n(t) \tag{3}$$

where $J(\cdot)$ denotes the contribution from NBI, $h(\cdot)$ is the channel impulse response, $\otimes$ represents the convolution operator, and $n(\cdot)$ is the zero–mean Additive White Gaussian Noise (AWGN) with two–sided power spectral density $N_0/2$.

The impulse response, $h(\cdot)$, of a generic UWB channel is [8]–[10]:

$$h(t) = \sum_{l=0}^{L-1} \alpha_l \delta(t - \tau_l) \tag{4}$$

where α_l and τ_l denote gain and delay of the l–path, respectively, L is the number of received multipath components, and $\delta(\cdot)$ is the Dirac's delta function. Moreover, $\{\alpha_l\}_{l=0}^{L-1} = \beta_l p_l$, where $\{\beta_l\}_{l=0}^{L-1}$ denotes the fading gain, which may be Nakagami–m, Log–Normal, Rice or Rayleigh distributed [42], and $\{p_l\}_{l=0}^{L-1}$ is a pulse polarity factor that takes values ± 1 with equal probability. For analytical tractability, intra–pulse interference is neglected in our analysis [69], *i.e.*, $|\tau_l - \tau_m| \geq T_w$, $\forall l \neq m$, where $\{\tau_l\}_{l=1}^{L-1} = \tau_0 + lT_w$. Moreover, to avoid Inter–Symbol (ISI) and Inter–Chip Interference (ICI), we consider $T_c \geq T_d$, where T_d denotes the maximum excess delay of the channel, *i.e.*, $T_d = \tau_{L-1} - \tau_0$. Furthermore, without loss of generality, we assume $\tau_0 = 0$.

As mentioned in Section I, we adopt a single– and multi–tone model for the NBI. As a consequence, if multiple jammers are simultaneously active over the transmission bandwidth of the UWB signal, $J(\cdot)$ in (3) reduces as follows:

$$J(t) = \sum_{k=1}^{N_I} \sqrt{2J_k}\alpha_{J_k} \cos(2\pi f_{J_k} t + \theta_{J_k}) \tag{5}$$

where N_I is the number of active jammers, and $\{J_k\}_{k=1}^{N_I}$, $\{\alpha_{J_k}\}_{k=1}^{N_I}$, $\{f_{J_k}\}_{k=1}^{N_I}$, $\{\theta_{J_k}\}_{k=1}^{N_I}$ are average received power, channel gain, carrier frequency, and phase of the interfering signals, respectively. Similar to [53], we assume a flat–fading and slowly–varying multipath channel model for each jammer.

C. Receiver Operations

As shown in Fig. 1, the received signal $r(\cdot)$ in (3) is passed through an ideal band–pass filter with bandwidth W and center frequency f_c to eliminate out–of–band noise and interference. We assume W is large enough to introduce a negligible distortion on both the shape of the received pulse and the in–band NBI. On the other hand, the noise autocorrelation function at the filter output is:

$$R_{\tilde{n}}(\tau) = WN_0 \mathrm{sinc}(\mathrm{W}\tau) \cos(2\pi f_c \tau) \tag{6}$$

where $\tilde{n}(\cdot)$ represents the filtered version of $n(\cdot)$, and $\mathrm{sinc}(x) = \sin(x)/x$.

After filtering, the signal $\tilde{r}(t) = (s \otimes h)(t) + J(t) + \tilde{n}(t)$ at the filter output is first multiplied by a T_c–delayed version of itself, and then weighted by a locally–generated gating waveform, $z(\cdot)$, which, for each $N_s T_c$–long signaling interval, is defined as follows:

$$z(t;\tau) = \sum_{j=0}^{N_s-1} c_j g(t - jT_c - \tau) \tag{7}$$

where[2] $g(t) = \mathrm{rect}(t/T_I - 0.5)$, $0 < T_I \leqslant T_c$ is the time integration window, $L_{\mathrm{cap}} = \lfloor T_I/T_w \rfloor$ is the number of captured multipath components in that window, and τ is a time delay between received signal and local template [42]. Finally, we emphasize that the local signal $z(\cdot)$ is independent of the transmitted and received pulse waveforms, but it is only used to de–spread the received signal and filter out noise and interference that lay outside the signal region.

D. Performance Measures

1) Data Detection: As far as data detection is concerned, the main performance metric to be computed is the ABEP. In particular, by assuming perfect bit synchronization at the receiver (*i.e.*, $\tau = 0$), the (soft) decision variable at the detector input for the i–th bit time is:

$$Q_i = \int_{iT_b}^{(i+1)T_b} \tilde{r}(t)\, \tilde{r}(t - T_c)\, z(t - iT_b)\, dt \tag{8}$$

By adopting the optimal decision rule for a single–user and interference–free system setup to keep the receiver complexity at a low level, the received bits are estimated as follows [37]:

$$\hat{b}_i = \mathrm{sign}(Q_i) \tag{9}$$

which leads to the following definition for the ABEP:

$$\mathrm{ABEP} = \Pr\left\{ b_i \neq \hat{b}_i \right\} \tag{10}$$

where $\mathrm{sign}(\cdot)$ is the sign function, *i.e.*, $\mathrm{sign}(x) = 1$ if $x \geq 0$ and $\mathrm{sign}(x) = -1$ if $x < 0$, and $\Pr\{\cdot\}$ denotes probability.

2) Timing Acquisition: As far as timing acquisition is concerned, the main performance metrics to be computed are $\mathrm{P_d}$ and $\mathrm{P_{fa}}$. In particular, by considering a generic $N_s T_c$–long observation window $t \in [\tau + iN_s T_c, \tau + (i+1) N_s T_c)$ for signal detection, and defining the (soft) decision variable at the detector input as follows:

$$D_i(\tau) = \int_{\tau + iN_s T_c}^{\tau + (i+1)N_s T_c} \tilde{r}(t)\, \tilde{r}(t - T_c)\, z(t - iN_s T_c; \tau)\, dt \tag{11}$$

$\mathrm{P_d}$ and $\mathrm{P_{fa}}$ can be defined as [49]:

$$\begin{cases} \mathrm{P_d} = \Pr\{ D_i(\tau) \geq \mathrm{D_{th}} | \, \tau = 0 \text{ and } s(\cdot) \neq 0 \} \\ \mathrm{P_{fa}} = \Pr\{ D_i(\tau) \geq \mathrm{D_{th}} | \, \tau = 0 \text{ and } s(\cdot) = 0 \} \end{cases} \tag{12}$$

where $\mathrm{D_{th}}$ is the detection threshold. In other words, $\mathrm{P_d}$ is the probability that $D_i(\cdot)$ is above $\mathrm{D_{th}}$ when the useful user is actually transmitting (*i.e.*, $s(\cdot) \neq 0$), while $\mathrm{P_{fa}}$ is the same probability but when there is no active useful user (*i.e.*, $s(\cdot) = 0$). Also, let us note that in (12) we have considered, similar to [49] and references therein, the system setup with $\tau = 0$. The framework described in this paper has been recently generalized in [70] for $\tau \neq 0$, but the analytical development is not reported here for two reasons: i)

[2] $\mathrm{rect}(t/2T) = 1$ if $-T \leq t \leq T$ and $\mathrm{rect}(t/2T) = 0$ elsewhere.

$$U_i = \int_{iT_b}^{(i+1)T_b} \left[(s \otimes h)(t) \cdot (s \otimes h)(t - T_c) \right] z(t - iT_b)\, dt = b_i N_s E_w \sum_{l=0}^{L_{\text{cap}}-1} \alpha_l^2 \tag{15}$$

$$\begin{aligned} I_i = & \underbrace{\int_{iT_b}^{(i+1)T_b} \left[J(t) \cdot (s \otimes h)(t - T_c) \right] z(t - iT_b)\, dt}_{I_i^{(1)}} + \underbrace{\int_{iT_b}^{(i+1)T_b} \left[J(t - T_c) \cdot (s \otimes h)(t) \right] z(t - iT_b)\, dt}_{I_i^{(2)}} \\ & + \underbrace{\int_{iT_b}^{(i+1)T_b} \left[J(t) \cdot J(t - T_c) \right] z(t - iT_b)\, dt}_{I_i^{(3)}} \cong J_1 T_I \alpha_{J_1}^2 \cos(2\pi f_{J_1} T_c) \sum_{j=0}^{N_s-1} c_j \end{aligned} \tag{16}$$

space constraints, and ii) because in [70] it is shown that the optimal code design is unaffected by the mistiming $\tau \neq 0$. In other words, the analytical development is much more involving, but the outcome about system optimization of the $\mathrm{T_c}$–DTR scheme is the same. Accordingly, we will omit the time–delay variable τ in the next sections. We also remark that, under this assumption, it can be readily verified that $D_i(\tau)|_{\tau=0} = Q_i|_{b_i=+1}\ \forall i$. So, in what follows, we will unify the analytical treatment of both decision metrics by taking into account this latter condition.

III. Performance Analysis: Single–Tone Interference

Moving from system model and receiver operation introduced in Section II, the aim of this section is to provide a simple but insightful analytical framework for analyzing the performance of the proposed $\mathrm{T_c}$–DTR transceiver over multipath fading channels with a single–tone NBI. Recently, some advanced analytical frameworks have been proposed to compute error and detection probabilities of TR receivers, which are based on the general theory of "sampling expansion" (see, *e.g.*, [37], [38], [42], [44], [49]). These methods are quite powerful, as they allow us to write the performance metric of interest in a form that is very conveniently expressed for computing the average over the distribution of the channel gains, without the need of Monte Carlo methods. Unlike these contributions, the main aim of this paper is to propose a framework with a different and twofold objective: i) the framework should be accurate but simple enough to be used for system optimization, and, more specifically, to identify the degrees of freedom to reduce the effect of interference; and ii) the framework should be accurate but insightful enough for a simple comparison among various receiver schemes based on the TR principle, as well as to readily understand advantages and disadvantages of each of them with regard to coexistence issues. In this paper, we show that using the Gaussian approximation for the cross–noise term is sufficient to derive the optimal code design and parameters setup to reduce the effect of interference, and to understand strengths and weaknesses of many receiver schemes. In fact, the proposed optimization method does not require closed–form expressions of the metrics of interest averaged over the fading distribution, but conditional (upon channel statistics) metrics are used. After optimization, the average performance metrics are computed using Monte Carlo methods. Finally, we emphasize that the Gaussian approximation is used only to model the cross–noise term arising from TR operations, no Gaussian approximations are considered to analytically modeling the tone interference.

A. Framework to Compute the ABEP

The ABEP is computed by using a three–step procedure: i) first, the (Signal+Interference)–to–Noise Ratio ((S+I)NR) is defined and computed, ii) second, the conditional (upon the channel coefficients of useful user and jammers) Bit Error Probability (BEP) is estimated, and iii) third, the ABEP is obtained via semi–analytical methods.

1) (S+I)NR: The decision variable in (8) can be written as the summation of three contributions U_i, I_i, and $\tilde{N}_i$ as follows:

$$Q_i = U_i + I_i + \tilde{N}_i \tag{13}$$

which are useful, interference, and noise terms, respectively.

The (S+I)NR conditioned upon the fading channels and the transmitted bits, $\gamma_i(\cdot,\cdot;\cdot)$, is defined as follows[3]:

$$\gamma_i\left(\{\alpha_l\}_{l=0}^{L_{\text{cap}}-1}, \alpha_{J_1}; b_i \right) = \frac{(U_i + I_i)^2}{\mathrm{E}\left\{ \tilde{N}_i^2 \right\}} = \frac{M_i^2}{\mathrm{E}\left\{ \tilde{N}_i^2 \right\}} \tag{14}$$

where $\mathrm{E}\{\cdot\}$ denotes the expectation operator computed over the AWGN.

After a few algebraic manipulations (see Appendix I for details and approximations), U_i and I_i in (13) can be re–written as shown in (15) and in (16) on top of this page, respectively, where the approximation in (16) is obtained by taking into account that, for typical system setups where $T_I \gg (4\pi f_{J_1})^{-1}$, we have $I_i^{(1)} + I_i^{(2)} \ll U_i + I_i^{(3)}$, and $I_i^{(3)} \cong J_1 T_I \alpha_{J_1}^2 \cos(2\pi f_{J_1} T_c) \sum_{j=0}^{N_s-1} c_j$. Further details can be found in Appendix I.

[3]With a slight inaccurate notation we highlight the conditioning only upon the channel gains of the NBI. The reason is that the simplified model presented in what follows depends only on these coefficients. The improved model in Section IV-B actually depends on other fading parameters as well. Moreover, we emphasize here that (14) implicitly assumes that $\mathrm{E}\left\{ \tilde{N}_i \right\} \cong 0$. This is actually true for all receiver architectures analyzed in this manuscript, except the ED. Further comments about this point can be found in Section VI, Table I, and Table II.

$$\begin{cases} P_b\left(\{\alpha_l\}_{l=0}^{L_{\rm cap}-1},\alpha_{J_1}\right)=0.5Q\left(\sqrt{\bar{\gamma}_i^{(-1)}}\right)+0.5Q\left(\sqrt{\bar{\gamma}_i^{(+1)}}\right) & \text{if} \quad M_i|_{b_i=-1}<0 \quad \text{and} \quad M_i|_{b_i=+1}\geq 0 \\ P_b\left(\{\alpha_l\}_{l=0}^{L_{\rm cap}-1},\alpha_{J_1}\right)=0.5\left[1-Q\left(\sqrt{\bar{\gamma}_i^{(-1)}}\right)\right]+0.5Q\left(\sqrt{\bar{\gamma}_i^{(+1)}}\right) & \text{if} \quad M_i|_{b_i=-1}\geq 0 \quad \text{and} \quad M_i|_{b_i=+1}\geq 0 \\ P_b\left(\{\alpha_l\}_{l=0}^{L_{\rm cap}-1},\alpha_{J_1}\right)=0.5Q\left(\sqrt{\bar{\gamma}_i^{(-1)}}\right)+0.5\left[1-Q\left(\sqrt{\bar{\gamma}_i^{(+1)}}\right)\right] & \text{if} \quad M_i|_{b_i=-1}<0 \quad \text{and} \quad M_i|_{b_i=+1}<0 \\ P_b\left(\{\alpha_l\}_{l=0}^{L_{\rm cap}-1},\alpha_{J_1}\right)=0.5\left[1-Q\left(\sqrt{\bar{\gamma}_i^{(-1)}}\right)\right]+0.5\left[1-Q\left(\sqrt{\bar{\gamma}_i^{(+1)}}\right)\right] & \text{if} \quad M_i|_{b_i=-1}\geq 0 \quad \text{and} \quad M_i|_{b_i=+1}<0 \end{cases} \tag{18}$$

$$\begin{cases} \mathrm{P_d}\left(\{\alpha_l\}_{l=0}^{L_{\rm cap}-1},\alpha_{J_1}\right)=Q\left(\left.\dfrac{\mathrm{D_{th}}-\mu_{D_i}\left(\{\alpha_l\}_{l=0}^{L_{\rm cap}-1},\alpha_{J_1}\right)}{\sigma_{D_i}\left(\{\alpha_l\}_{l=0}^{L_{\rm cap}-1},\alpha_{J_1}\right)}\right| s(\cdot)\neq 0\right)=Q\left(\dfrac{\mathrm{D_{th}}-[U_i+I_i]}{\sqrt{\mathrm{E}\left\{\tilde{N}_i^2\right\}}}\right) \\ \mathrm{P_{fa}}\left(\{\alpha_l\}_{l=0}^{L_{\rm cap}-1},\alpha_{J_1}\right)=Q\left(\left.\dfrac{\mathrm{D_{th}}-\mu_{D_i}\left(\{\alpha_l\}_{l=0}^{L_{\rm cap}-1},\alpha_{J_1}\right)}{\sigma_{D_i}\left(\{\alpha_l\}_{l=0}^{L_{\rm cap}-1},\alpha_{J_1}\right)}\right| s(\cdot)=0\right)=Q\left(\dfrac{\mathrm{D_{th}}-I_i}{\sqrt{\mathrm{E}\left\{\tilde{N}_i^2\right\}\big|_{E_w=0}}}\right) \end{cases} \tag{21}$$

Moreover, the noise power, $\mathrm{E}\left\{\tilde{N}_i^2\right\}$, is:

$$\begin{aligned} \mathrm{E}\left\{\tilde{N}_i^2\right\} \cong\ & N_0\left(2N_s-1\right)E_w\sum_{l=0}^{L_{\rm cap}-1}\alpha_l^2 \\ & +0.5N_0^2N_sWT_I+N_0N_sJ_1T_I\alpha_{J_1}^2 \\ & +N_0J_1T_I\alpha_{J_1}^2\cos\left(4\pi f_{J_1}T_c\right)\sum_{j=1}^{N_s-1}c_jc_{j-1} \end{aligned} \tag{17}$$

which is obtained by following the same approach as in [29] and [71] but including DS coding and NBI. See also Appendix I for further information.

As a consequence, from (15)–(17) the (S+I)NR in (14) can be computed in closed–form.

2) BEP: The BEP, $P_b(\cdot,\cdot)$, can be easily obtained from $\gamma_i(\cdot,\cdot;\cdot)$ in (14) by relying on typical methods used to analyze the performance of wireless channels with ISI and Multiple Access Interference (MUI), which are based on the so–called "open–eye" method [72]. In particular, according to the decision rule in (9), four different cases need to be considered to accurately computing the error probability without resorting to the typical Gaussian approximation to account for the NBI. These four cases are shown in (18) on top of this page, where $Q(x)=\left(1/\sqrt{2\pi}\right)\int_x^{+\infty}\exp\left(-t^2/2\right)dt$ and, for notational simplicity, we have defined $\bar{\gamma}_i^{(\pm 1)}=\gamma_i\left(\{\alpha_l\}_{l=0}^{L_{\rm cap}-1},\alpha_{J_1};\pm 1\right)$. Furthermore, $M_i|_{b_i}$ is M_i in (14) when conditioning upon the transmission of the information bit b_i.

3) ABEP: The BEP in (18) is conditioned upon the fading statistics of UWB, $\{\alpha_l\}_{l=0}^{L_{\rm cap}-1}$, and NBI, α_{J_1}, channels. The ABEP can be readily computed by numerically averaging (18) over the distributions of $\{\alpha_l\}_{l=0}^{L_{\rm cap}-1}$ and α_{J_1}, as follows:

$$\mathrm{ABEP}=\mathrm{E}_{\{\alpha_l\}_{l=0}^{L_{\rm cap}-1},\alpha_{J_1}}\left\{P_b\left(\{\alpha_l\}_{l=0}^{L_{\rm cap}-1},\alpha_{J_1}\right)\right\} \tag{19}$$

where $\mathrm{E}_{\{\alpha_l\}_{l=1}^{L_{\rm cap}},\alpha_{J_1}}\{\cdot\}$ is the expectation operator computed over channel statistics.

B. Framework to Compute $\mathrm{P_d}$ *and* $\mathrm{P_{fa}}$

$\mathrm{P_d}$ and $\mathrm{P_{fa}}$ can be computed by using a procedure similar to that already used to compute the ABEP in Section III-A: i) first, the decision variable in (11) is approximated with a Gaussian distributed Random Variable (RV) when conditioning upon fading channel statistics[4], ii) second, the conditional (upon the channel coefficients of useful user and jammers) $\mathrm{P_d}$ and $\mathrm{P_{fa}}$ are estimated, and iii) third, a semi–analytical method is used to remove the conditioning over the wireless channel.

1) Mean and Variance of D_i*:* By assuming D_i in (11) conditional Gaussian, its distribution is univocally determined by its mean, $\mu_{D_i}(\cdot,\cdot)$, and variance, $\sigma_{D_i}^2(\cdot,\cdot)$, which can be written as follows[5]:

$$\begin{cases} \mu_{D_i}\left(\{\alpha_l\}_{l=0}^{L_{\rm cap}-1},\alpha_{J_1}\right)=U_i+I_i \\ \sigma_{D_i}^2\left(\{\alpha_l\}_{l=0}^{L_{\rm cap}-1},\alpha_{J_1}\right)=\mathrm{E}\left\{\tilde{N}_i^2\right\} \end{cases} \tag{20}$$

where U_i, I_i, and $\tilde{N}_i$ can be found in (15)–(17) with $\{b_i\}_{i=-\infty}^{+\infty}=+1$ and $T_b=N_sT_c$, as described in Section II-D.2.

2) Conditional $\mathrm{P_d}$ *and* $\mathrm{P_{fa}}$*:* By exploiting again the "open–eye" method for performance analysis, it can be shown that, when conditioning upon fading channel statistics, $\mathrm{P_d}$ and $\mathrm{P_{fa}}$ can be computed as shown in (21) on top of this page, where we have taken into account that to compute $\mathrm{P_{fa}}$ the contribution from the useful user has to be removed in (15)–(17): *i.e.*, $U_i=0$ and when computing $\mathrm{E}\left\{\tilde{N}_i^2\right\}$ we have to set $E_w=0$.

[4]We emphasize again that the Gaussian approximation is for the cross–noise term only and is not used for the NBI.

[5]Similar to (14), also (20) assumes that $\mathrm{E}\left\{\tilde{N}_i\right\}\cong 0$.

$$I_i \cong I_i^{(3)} = \sum_{j=0}^{N_s-1} \left\{ c_j \int_0^{T_I} \left[\left(\sum_{k=1}^{N_I} \zeta_{k,j}\left(t\right) \right) \left(\sum_{h=1}^{N_I} \zeta_{h,j}\left(t - T_c\right) \right) \right] dt \right\} \tag{25}$$

$$\begin{aligned} I_i \cong I_i^{(3)} = & \sum_{k=1}^{N_I} \left[J_k \alpha_{J_k}^2 \cos\left(2\pi f_{J_k} T_c\right) \right] \left(T_I \sum_{j=0}^{N_s-1} c_j \right) + \sum_{j=0}^{N_s-1} \left\{ c_j \sum_{k=1}^{N_I} \left[\int_0^{T_I} J_k \alpha_{J_k}^2 \cos\left(4\pi f_{J_k}\left(t + jT_c - 0.5T_c\right) + 2\theta_{J_k}\right) dt \right] \right\} \\ & + \sum_{j=0}^{N_s-1} \left\{ c_j \sum_{k=1}^{N_I} \sum_{h\neq k=1}^{N_I} \left[\int_0^{T_I} \sqrt{J_k J_h} \alpha_{J_k} \alpha_{J_h} \cos\left(2\pi\left(f_{J_k} + f_{J_h}\right)\left(t + jT_c\right) - 2\pi f_{J_h} T_c + 2\left(\theta_{J_k} + \theta_{J_h}\right)\right) dt \right] \right\} \\ & + \sum_{j=0}^{N_s-1} \left\{ c_j \sum_{k=1}^{N_I} \sum_{h\neq k=1}^{N_I} \left[\int_0^{T_I} \sqrt{J_k J_h} \alpha_{J_k} \alpha_{J_h} \cos\left(2\pi\left(f_{J_k} - f_{J_h}\right)\left(t + jT_c\right) + 2\pi f_{J_h} T_c + 2\left(\theta_{J_k} - \theta_{J_h}\right)\right) dt \right] \right\} \end{aligned} \tag{26}$$

3) $\mathrm{P_d}$ *and* $\mathrm{P_{fa}}$*:* Finally, similar to (19), $\mathrm{P_d}$ and $\mathrm{P_{fa}}$ can be obtained by using a semi–analytical method as follows:

$$\begin{cases} \mathrm{P_d} = \mathrm{E}_{\left\{\alpha_l\right\}_{l=0}^{L_{\mathrm{cap}}-1}, \alpha_{J_1}} \left\{ \mathrm{P_d}\left(\left\{\alpha_l\right\}_{l=0}^{L_{\mathrm{cap}}-1}, \alpha_{J_1} \right) \right\} \\ \mathrm{P_{fa}} = \mathrm{E}_{\left\{\alpha_l\right\}_{l=0}^{L_{\mathrm{cap}}-1}, \alpha_{J_1}} \left\{ \mathrm{P_{fa}}\left(\left\{\alpha_l\right\}_{l=0}^{L_{\mathrm{cap}}-1}, \alpha_{J_1} \right) \right\} \end{cases} \tag{22}$$

IV. Performance Analysis: Multi–Tone Interference

Let us now consider the scenario with $N_I > 1$. In this case, the analysis is more involving with respect to the setup with a single–tone NBI. Due to space constraints, we do not report all the details of the analytical derivation, but we summarize only the final results. In particular, the development is heavily based on the analytical derivation described in detail in Section III for $N_I = 1$.

More specifically, the final expressions of the ABEP in (18) and (19), as well as $\mathrm{P_d}$ and $\mathrm{P_{fa}}$ in (21) and (22) can be still applied by taking into consideration that: i) (18) and (21) are conditioned upon the set of channel gains $\left\{\alpha_{J_k}\right\}_{k=1}^{N_I}$, and ii) (19) and (22) need to be averaged over the channel gain of each jammer. Accordingly, for all performance metrics only the terms I_i, $\tilde{N}_i$ in (13) need to be modified to account for multiple interfering jammers. In what follows, two approximation methods are proposed to this end:

1) The first method is based on the approximation that the jammers sum up in power in I_i, $\tilde{N}_i$.
2) The second method yields a more accurate, but more complicated, approximation that considers all contributions actually present in I_i.

In Section VII, we will see that the first method is accurate for moderately low SIRs, while it starts being less accurate when each active jammer is very strong (*i.e.*, low SIRs). On the other hand, we will verify that the second method is reasonably accurate for low SIRs as well.

A. Simple Approximation

By assuming that all contributions coming from NBI sum up in power, I_i, $\tilde{N}_i$ in (13) can be generalized as follows, respectively:

$$I_i \cong I_i^{(3)} \cong \sum_{k=1}^{N_I} \left[J_k \alpha_{J_k}^2 \cos\left(2\pi f_{J_k} T_c\right) \right] \left(T_I \sum_{j=0}^{N_s-1} c_j \right) \tag{23}$$

$$\begin{aligned} \mathrm{E}\left\{ \tilde{N}_i^2 \right\} \cong & N_0 \left(2N_s - 1\right) E_w \sum_{l=0}^{L_{\mathrm{CAP}}-1} \alpha_l^2 + 0.5 N_0^2 N_s W T_I \\ & + N_0 N_s T_I \sum_{k=1}^{N_I} J_k \alpha_{J_k}^2 \\ & + N_0 T_I \sum_{k=1}^{N_I} \left[J_k \alpha_{J_k}^2 \cos\left(4\pi f_{J_k} T_c\right) \right] \left(\sum_{j=1}^{N_s-1} c_j c_{j-1} \right) \end{aligned} \tag{24}$$

The interested reader can obtain (23) and (24) by following the same analytical steps already described in Appendix I.

B. Improved Approximation

The improved approximation stems from the consideration that, for low SIRs, the terms in I_i arising from the cross–products among the jammers could have a non–negligible contribution. On the other hand, we have empirically found (see also Section VII) that the same cross–products have a less pronounced effect in $\tilde{N}_i$, since the error floor in all performance metrics considered in this paper is mainly caused by I_i. This claim will be better substantiated in Section V and Section VII. Further comments and details can be found in [73].

In particular, I_i can be approximated as shown in (25) on top of this page, where we have defined $\left\{ \left\{ \zeta_{k,j}\left(t\right) \right\}_{k=1}^{N_I} \right\}_{j=0}^{N_s-1} = \sqrt{2J_k} \alpha_{J_k} \cos\left(2\pi f_{J_k}\left(t + jT_c\right) + \theta_{J_k}\right)$. Furthermore, after some simple algebraic manipulations, (25) can be explicitly re–written as shown in (26) on top of this page. We note that the first term in (26) corresponds to the approximation in (23), while the last three contributions account for the actual coherent summation of the jammers. The last two addends depend on the summation and on the difference

$$\begin{cases} \mathrm{C}_1: & \displaystyle\sum_{j=0}^{N_s-1} c_j = 0 \\ \mathrm{C}_2: & \displaystyle\sum_{j=1}^{N_s-1} c_j c_{j-1} = -N_s \left[\sum_{k=1}^{N_I} J_k \mathrm{E}\left\{\alpha_{J_k}^2\right\}\right] \left[\sum_{k=1}^{N_I} J_k \mathrm{E}\left\{\alpha_{J_k}^2\right\} \cos\left(4\pi f_{J_k} T_c\right)\right]^{-1} \end{cases} \tag{28}$$

between pairs of jammer frequencies, respectively. According to the discussions in Section III and Appendix I, it follows that the last addend is expected to yield a more significant contribution for low SIRs.

Finally, we notice that other terms in I_i (*i.e.*, $I_i^{(1)}$, and $I_i^{(2)}$ in (16)) might have a non–negligible contribution for low SIRs. However, the analysis in Appendix I has evidenced that these terms could be made arbitrarily small via pulse shaping methods, *i.e.*, by introducing notches in each frequency where a jammer is transmitting. Further details about this point can be found in Section V. We note that while proper pulse shaping might be a good method for interference rejection for coherent UWB receivers [53], this is, in general, not sufficient for TR schemes because of the non–linear processing at the receiver, which causes the cross–interference term (see, *e.g.*, (16)).

V. System Optimization: Optimal Code Design

Let us now exploit the frameworks introduced in Section III and Section IV to derive the optimal system design to minimize the effect of NBI for both single– and multi–tone scenarios. In particular, the main objective of this section is to look into the performance metrics with the purpose of identifying the relations among the system parameters, *e.g.*, DS code, chip–time, pulse waveform, that can be adequately tuned to guaranteeing a higher robustness to NBI. The ultimate goal is the development of closed–form (approximate) formulas, which provide insights and precise design guidelines on how to best choose the degrees of freedom of the system to reduce, as much as possible, the effect of NBI, which is explicitly present in the final expressions of the performance metrics of interest. Also, we are interested in highlighting the amount of side information, *i.e.*, channel– and interference–awareness, needed for a practical implementation of these formulas.

As far as the single–tone scenario is concerned, from (16) and (17) it follows that NBI can be completely eliminated if the following two conditions are verified simultaneously:

$$\begin{cases} \mathrm{C}_1: & \displaystyle\sum_{j=0}^{N_s-1} c_j = 0 \\ \mathrm{C}_2: & \displaystyle\sum_{j=1}^{N_s-1} c_j c_{j-1} = -N_s \left[\cos\left(4\pi f_{J_1} T_c\right)\right]^{-1} \end{cases} \tag{27}$$

which is the optimal code design to reduce the NBI for all performance metrics studied in this paper.

In particular: i) C_1 simply states that the DS code should be perfectly balanced, and ii) C_2 suggests to design a DS code with an auto–correlation function evaluated at T_c equal to $-N_s/\cos\left(4\pi f_{J_1} T_c\right)$. Moreover, while C_1 is independent of the characteristics of the NBI (*e.g.*, the jammer carrier frequency), C_2 requires the knowledge of f_{J_1}. In Section VII, we will show that the most important condition for system optimization and NBI rejection is C_1. Moreover, let us emphasize that while C_1 can always be satisfied via a proper code design, C_2 cannot be exactly satisfied as it involves the *partial* correlation function of the DS code, which can be at the most equal to $\pm(N_s-1)$, while the absolute value of the right hand side of C_2 is always greater than N_s. However, the DS code can always be designed in order to minimize the difference between the left and right hand sides of C_2: *i.e.*, the condition C_2 can be approximately achieved.

It is very interesting to note that a code design similar to C_1 has been recently developed in [74] for the original delay–hopped TR scheme [3]. In particular, [74, Eq. (35)] coincides with C_1 in (27) for unit–length TH codes. Also, similar to C_1, [74, Eq. (35)] is independent of the jammer carrier frequency. In spite of these similarities, there are many differences between the code design proposed in this paper and [74]. In particular: i) the delay–hopped TR scheme in [74] is more complicated to be implemented in practice with respect to our $\mathrm{T_c}$–DTR detector. As a matter of fact, it needs a number of delay lines equal to the length of the TH code, while the $\mathrm{T_c}$–DTR scheme requires just a single delay line; ii) to reduce the effect of NBI, all these delay lines must be properly tuned, while C_1 is independent of the length of the delay line, *i.e.*, the chip–time; and, more importantly, iii) the optimization problem studied in [74] neglects the AWGN, which, on the other hand, is well tackled by C_2 in (27), which, as we will better show in Section VI, is the main distinguishable feature and reason for the $\mathrm{T_c}$–DTR scheme to achieve better performance with respect to state–of–the–art TR schemes. A common characteristic of C_1 in (27) and [74, Eq. (35)] is that they both require the DS code to be perfectly balanced for interference rejection.

As far as the multi–tone scenario is concerned, the conditions that the DS code should satisfy to reduce the effect of NBI can be derived, *e.g.*, from (23) and (24) by considering the assumptions that all the jammers sum up incoherently. However, an important consideration is worth being made in this case. The condition C_2 in (27) allows us to *deterministically* cancel out the jammer falling within the transmission bandwidth of the UWB useful signal, since (27) is independent of the channel gain, α_{J_1}, and phase, θ_{J_1}. On the other hand, from (24) it seems very complicated, for arbitrary values of carrier frequencies of the interferers, that a similar condition can be achieved for the multi–tone scenario. Mathematically speaking, it seems very difficult to design a code that satisfies the condition $\sum_{k=1}^{N_I}\left[J_k\alpha_{J_k}^2\cos\left(4\pi f_{J_k}T_c\right)\right]\left(\sum_{j=1}^{N_s-1}c_jc_{j-1}\right) = -N_s\sum_{k=1}^{N_I}J_k\alpha_{J_k}^2$ for any single realization of the channel

statistics. For this reason, in this paper we propose a code design that can cancel out *statistically*, *i.e.*, on average, the NBI in a multi–tone scenario. Accordingly, from (23) and (24) the conditions for code design in (28) on top of the previous page can be obtained, where C_1 is the same as in (27).

Furthermore, we note that for those system setups where the framework in Section IV-A is inaccurate, the condition C_1 in (28) should be replaced by a similar optimization criterion that could be obtained from (26). With similar arguments as those already described for C_2 in (28), the new condition can be concisely written as $\mathrm{E}\{I_i\} \cong \mathrm{E}\left\{I_i^{(3)}\right\} = 0$. Due to the complexity of the latter optimization criterion, we will not consider it for performance optimization in this paper. As a matter of fact, even though C_1 in (28) might not be optimal for some system setups, it still allows us to reduce the effect of the NBI for all system scenarios. This claim is substantiated by the fact that the first addend in (26) is exactly (23), from which C_1 in (28) has been derived.

Finally, two remarks are worth being made about the design criteria for optimizing the performance of the $\mathrm{T_c}$–DTR receiver. 1) The first comment is concerned with C_2 in (27) and (28). It is important to note that C_2 foresees a joint optimization of DS code and chip–time T_c, which needs to be carefully chosen by also reducing the effect of ISI and ICI due to the frequency–selectivity of the UWB channel. 2) The second comment is related to the possibility to tune other parameters at the transmitter for performance optimization. A simple way to reduce further the effect of the NBI is to properly design the shape of the transmitted pulse. This remark follows from (30) and (33) in Appendix I, where it is shown that having frequency notches near the carrier frequencies of the jammers can help reducing the effect of NBI. This comment applies to other non–coherent receiver architectures as well [41], [73].

VI. Comparison with other Non–Coherent Receiver Schemes

In this section, we compare the performance of the $\mathrm{T_c}$–DTR scheme with other relevant non–coherent receivers proposed in the literature. The study aims at highlighting advantages and disadvantages of each receiver scheme, and at showing the inherent robustness and flexibility of the $\mathrm{T_c}$–DTR receiver. In particular, TR [38], DTR [38], ED [39], Code–Multiplexed TR (CM–TR) [12], and $\mathrm{T_c}$–DTR receiver architectures are analyzed in this section. We emphasize here that the performance of the CM–TR receiver in the presence of NBI has never been studied in the literature, either by simulation or by analytical modeling. Furthermore, most performance studies are restricted to a limited number of receiver schemes, and, very often, consider only the ABEP (see, *e.g.*, the recent paper [45] and references therein). These are two additional and important contributions of the present paper.

Let us consider the scenario with a single–tone NBI. The setup with multi–tone NBI is addressed at the end of this section. For a simple comparison, we have summarized, for various receiver architectures, in Table I and in Table II the performance metrics needed to compute ABEP, $\mathrm{P_d}$ and $\mathrm{P_{fa}}$, as described in Section III. In particular, the results shown in Table I and in Table II for TR, DTR, ED, and CM–TR[6] receivers have been obtained by using the same approach described in Section III. However, the details of the derivation are here omitted, but can be found in [73]. Unlike [38] and [39], these results have been obtained by resorting to the Gaussian approximation for the cross–noise term. The agreement with the frameworks in [38], [39] has been verified in [73]. The framework for the CM–TR[7] receiver is not available elsewhere.

By carefully comparing the analytical models in Table I and in Table II, the following comments can be made. i) As far as the ABEP is concerned, previous results (see, *e.g.*, [41]) have shown that the ED outperforms both TR and DTR schemes in scenarios with strong NBI. In fact, it exploits an orthogonal modulation scheme (*i.e.*, Pulse Position Modulation, PPM) to cancel out the dominant part of the NBI term in the numerator of $\gamma_i(\cdot,\cdot;\cdot)$. However, this property no longer holds as far as $\mathrm{P_d}$ and $\mathrm{P_{fa}}$ are concerned. Since only an unmodulated train of pulses is transmitted in this latter case, the I_i term of the ED scheme is similar to that of TR and DTR receivers: this leads to a similar behavior of all receivers for low SIRs, and it is the main responsible for the dramatic performance worsening in such scenarios, as we will show in Section VII. ii) As far as TR (for ABEP, $\mathrm{P_d}$ and $\mathrm{P_{fa}}$), DTR (for ABEP, $\mathrm{P_d}$ and $\mathrm{P_{fa}}$), and ED (for $\mathrm{P_d}$ and $\mathrm{P_{fa}}$) receivers are concerned, the performance floor for strong NBI and high SNRs (Signal–to–Noise–Ratios) is mainly due to the $N_s J_1 T_I \alpha_{J_1}^2 \cos(2\pi f_{J_1} T_r)$, $N_s J_1 T_I \alpha_{J_1}^2 \cos(2\pi f_{J_1} T_b)$, and $N_s J_1 T_I \alpha_{J_1}^2$ terms in the numerator of $\gamma_i(\cdot,\cdot;\cdot)$ and in I_i, respectively. iii) As far as the CM–TR scheme is concerned, we notice that the transmission of reference and data signals over two orthogonal codes allows it to reject the contribution of the NBI in the numerator of $\gamma_i(\cdot,\cdot;\cdot)$ and in I_i. So, when $\mathrm{P_d}$ and $\mathrm{P_{fa}}$ are considered, it turns out to be more robust to NBI than the ED detector. Moreover, since the CM–TR receiver uses an amplitude modulation scheme instead of a position modulation scheme, it offers approximately 1.5dB of performance gain over the AWGN channel with respect to the ED receiver. iv) As far as TR and DTR receivers are concerned, the terms in ii) can be, in principle, canceled out by designing T_r and T_b to satisfy the conditions $\cos(2\pi f_{J_1} T_r) = 0$ and $\cos(2\pi f_{J_1} T_b) = 0$, respectively. However, this foresees the knowledge of the carrier frequency, f_{J_1}, of the interfering signal. Furthermore, as far as the ED is considered, Table II clearly shows that I_i can never be reduced to zero in this case. The optimization conditions about T_r and T_b for TR and DTR receivers, respectively, are very similar to [74, Eq. (35)]. In fact, in that paper the delays are properly tuned to reduce to zero the mean value of the interference at the

[6]Note that, with a slight abuse of notation, as far as the ED is concerned we have included in U_i the non–zero mean value of the noise term at the integrator output. As a matter of fact, we have already mentioned in Section III-A.1 that the ED is the only receiver studied in this paper with $\mathrm{E}\left\{\tilde{N}_i\right\} \neq 0$.

[7]Note that, when neglecting the NBI, our analytical framework is slightly different from [12] because we have taken into account that the available transmit–power is split between data and reference codewords: this allows us to perform a fair comparison among all the receiver schemes [41].

TABLE I

(S+I)NR OF THE DECISION VARIABLE OF NON–COHERENT RECEIVER SCHEMES WITH SINGLE–TONE NBI. THE SYMBOLS ARE DEFINED IN [38] FOR TR AND DTR, IN [39] FOR ED, AND IN [12] FOR CM–TR RECEIVERS. AS FAR AS THE CM–TR RECEIVER IS CONCERNED, THE MULTIPLEXING CODES ARE ASSUMED TO SATISFY THE CONDITION IN [12, EQ. (8)].

Average Bit Error Probability (ABEP)	
Receiver	$\gamma_i\left(\cdot,\cdot;\cdot\right)$
TR	$\dfrac{\left(0.5b_iN_sE_w\sum\limits_{l=0}^{L_{\rm cap}-1}\alpha_l^2+N_sJ_1T_I\alpha_{J_1}^2\cos\left(2\pi f_{J_1}T_r\right)\right)^2}{0.5N_0N_sE_w\sum\limits_{l=0}^{L_{\rm cap}-1}\alpha_l^2+0.5N_0^2N_sWT_I+N_0N_sJ_1T_I\alpha_{J_01}^2}$
DTR	$\dfrac{\left(b_iN_sE_w\sum\limits_{l=0}^{L_{\rm cap}-1}\alpha_l^2+N_sJ_1T_I\alpha_{J_1}^2\cos\left(2\pi f_{J_1}T_b\right)\right)^2}{N_0N_sE_w\sum\limits_{l=0}^{L_{\rm cap}-1}\alpha_l^2+0.5N_0^2N_sWT_I+N_0N_sJ_1T_I\alpha_{J_1}^2}$
ED	$\dfrac{\left(N_sE_w\sum\limits_{l=0}^{L_{\rm cap}-1}\alpha_l^2\right)^2}{2N_0N_sE_w\sum\limits_{l=0}^{L_{\rm cap}-1}\alpha_l^2+2N_0^2N_sWT_I+4N_0N_sJ_1T_I\alpha_{J_1}^2}$
CM–TR	$\dfrac{\left(b_iN_sE_w\sum\limits_{l=0}^{L_{\rm cap}-1}\alpha_l^2\right)^2}{2N_0N_sE_w\sum\limits_{l=0}^{L_{\rm cap}-1}\alpha_l^2+N_0^2N_sWT_I+2N_0N_sJ_1T_I\alpha_{J_1}^2}$
$\mathrm{T_c}$–DTR	$\dfrac{\left(b_iN_sE_w\sum\limits_{l=0}^{L_{\rm cap}-1}\alpha_l^2+J_1T_I\alpha_{J_1}^2\cos\left(2\pi f_{J_1}T_c\right)\sum\limits_{j=0}^{N_s-1}c_j\right)^2}{N_0(2N_s-1)E_w\sum\limits_{l=0}^{L_{\rm cap}-1}\alpha_l^2+0.5N_0^2N_sWT_I+N_0N_sJ_1T_I\alpha_{J_1}^2+N_0J_1T_I\alpha_{J_1}^2\cos\left(4\pi f_{J_1}T_c\right)\sum\limits_{j=1}^{N_s-1}c_jc_{j-1}}$

output of the integrator. The conditions $\cos\left(2\pi f_{J_1}T_r\right)=0$ and $\cos\left(2\pi f_{J_1}T_b\right)=0$ do the same. However, there is an important difference about the a priori information needed by the decoder for this optimization. For TR and DTR schemes, the carrier frequency of the jammer must be known to compute the best T_r and T_b. On the other hand, the delay–hopped TR scheme in [74] exploits the many available delay lines to conceive an optimization strategy that is oblivious to the frequency of the interferer. Thus, we can notice that a trade–off exists: multiple delay lines avoid the need to estimate the frequency of the jammer, but a receiver scheme with many delay lines is more complicated to be implemented in practice. v) For all receivers (apart from the $\mathrm{T_c}$–DTR), the contribution of the NBI in the denominator of $\gamma_i\left(\cdot,\cdot;\cdot\right)$ for the ABEP and in $\mathrm{E}\left\{\tilde{N}_i^2\right\}$ for $\mathrm{P_d}$ and $\mathrm{P_{fa}}$ cannot be straightforwardly canceled out without resorting to additional signal processing operations (see, *e.g.*, [64]), but it always introduces a performance penalty that increases with the power of the interferers.

On the contrary, by looking at Table I and at Table II we can readily observe that the $\mathrm{T_c}$–DTR receiver offers more degrees of freedom to reject the NBI via a simple design of some system parameters. i) First, we observe that if C_1 is verified, it offers the same robustness as the ED and CM–TR solutions when the ABEP is the performance metric of interest: the contribution of the NBI in the numerator of $\gamma_i\left(\cdot,\cdot;\cdot\right)$ can be removed. Furthermore, the $\mathrm{T_c}$–DTR receiver is superior to the ED scheme when $\mathrm{P_d}$ and $\mathrm{P_{fa}}$ are the performance metrics of interest: I_i cannot be canceled out for this latter receiver. ii) Second, if C_2 is closely verified, the NBI can be almost completely removed from $\gamma_i\left(\cdot,\cdot;\cdot\right)$ and $\mathrm{E}\left\{\tilde{N}_i^2\right\}$, and among the solutions analyzed in Table I and in Table II, the $\mathrm{T_c}$–DTR scheme is the only receiver architecture that can easily provide a way to cancel out the contribution of the NBI in the denominator of $\gamma_i\left(\cdot,\cdot;\cdot\right)$ and in $\mathrm{E}\left\{\tilde{N}_i^2\right\}$: this results in a substantial performance gain for strong NBI. iii) From all the above, it follows that the $\mathrm{T_c}$–DTR scheme is the only receiver potentially offering, for all metrics of interest, almost NBI–free performance via a simple code design.

Furthermore, as far as the ABEP is concerned, let us consider, *e.g.*, the worst–case system setup

TABLE II

MEAN AND VARIANCE OF THE DECISION VARIABLE OF NON–COHERENT RECEIVER SCHEMES WITH SINGLE–TONE NBI. THE SYMBOLS ARE DEFINED IN [38] FOR TR AND DTR, IN [39] FOR ED, AND IN [12] FOR CM–TR RECEIVERS. AS FAR AS THE CM–TR RECEIVER IS CONCERNED, THE MULTIPLEXING CODES ARE ASSUMED TO SATISFY THE CONDITION IN [12, EQ. (8)].

Detection Probability ($\mathrm{P_d}$)	
Receiver	U_i, I_i, and $E\left\{\tilde{N}_i^2\right\}$
TR	$U_i = 0.5N_sE_w\sum_{l=0}^{L_{\mathrm{cap}}-1}\alpha_l^2$ $I_i = N_sJ_1T_I\alpha_{J_1}^2\cos\left(2\pi f_{J_1}T_r\right)$ $\mathrm{E}\left\{\tilde{N}_i^2\right\} = 0.5N_0N_sE_w\sum_{l=0}^{L_{\mathrm{cap}}-1}\alpha_l^2 + 0.5N_0^2N_sWT_I + N_0N_sJ_1T_I\alpha_{J_1}^2$
DTR	$U_i = N_sE_w\sum_{l=0}^{L_{\mathrm{cap}}-1}\alpha_l^2$ $I_i = N_sJ_1T_I\alpha_{J_1}^2\cos\left(2\pi f_{J_1}T_b\right)$ $\mathrm{E}\left\{\tilde{N}_i^2\right\} = N_0N_sE_w\sum_{l=0}^{L_{\mathrm{cap}}-1}\alpha_l^2 + 0.5N_0^2N_sWT_I + N_0N_sJ_1T_I\alpha_{J_1}^2$
ED	$U_i = N_sE_w\sum_{l=0}^{L_{\mathrm{cap}}-1}\alpha_l^2 + N_0N_sWT_I$ $I_i = N_sJ_1T_I\alpha_{J_1}^2$ $\mathrm{E}\left\{\tilde{N}_i^2\right\} = 2N_0N_sE_w\sum_{l=0}^{L_{\mathrm{cap}}-1}\alpha_l^2 + N_0^2N_sWT_I + 2N_0N_sJ_1T_I\alpha_{J_1}^2$
CM–TR	$U_i = N_sE_w\sum_{l=0}^{L_{\mathrm{cap}}-1}\alpha_l^2$ $I_i = 0$ $\mathrm{E}\left\{\tilde{N}_i^2\right\} = 2N_0N_sE_w\sum_{l=0}^{L_{\mathrm{cap}}-1}\alpha_l^2 + N_0^2N_sWT_I + 2N_0N_sJ_1T_I\alpha_{J_1}^2$
$\mathrm{T_c}$–DTR	$U_i = N_sE_w\sum_{l=0}^{L_{\mathrm{cap}}-1}\alpha_l^2$ $I_i = J_1T_I\alpha_{J_1}^2\cos\left(2\pi f_{J_0}T_c\right)\sum_{j=1}^{N_s-1}c_j$ $\mathrm{E}\left\{\tilde{N}_i^2\right\} = N_0\left(2N_s-1\right)E_w\sum_{l=0}^{L_{\mathrm{cap}}-1}\alpha_l^2 + 0.5N_0^2N_sWT_I$ $+N_0N_sJ_1T_I\alpha_{J_1}^2 + N_0J_1T_I\alpha_{J_1}^2\cos\left(4\pi f_{J_1}T_c\right)\sum_{j=1}^{N_s-1}c_jc_{j-1}$

$\cos(4\pi f_{J_1} T_c) \sum_{j=1}^{N_s-1} c_j c_{j-1} = N_s - 1$. The following comments hold in this case. i) When ED and $\mathrm{T_c}$–DTR receivers are subject to the same average interference power, J_1, the $\mathrm{T_c}$–DTR scheme still outperforms the ED solution of 1.5dB (low SIRs) or 3dB (high SIRs), by also doubling the transmission data rate, given that no orthogonal modulation schemes (*i.e.*, PPM [39]) are required to reduce the contribution of the interference. ii) When ED and $\mathrm{T_c}$–DTR receivers are subject to the same SIR, which is defined as $\mathrm{SIR} = N_s E_w/(J_1 N_s T_c)$ (the chip–time of ED is twice the chip–time of $\mathrm{T_c}$–DTR), the $\mathrm{T_c}$–DTR solution offers the same performance as the ED scheme (low SIRs), but for a double transmission data rate. iii) When CM–TR and $\mathrm{T_c}$–DTR receivers are compared, the latter is 1.5dB better than the former for high SIRs and yields almost the same ABEP for low SIRs. In this case, data rate and chip–time are the same for both receivers. In conclusion, provided that $\mathrm{C_1}$ is satisfied, the $\mathrm{T_c}$–DTR scheme always provides some performance benefits with respect other non–coherent receiver schemes, even for the worst–case system setup.

Finally, let us consider the multi–tone reference scenario. Table I and Table II can be readily generalized by considering either (23) and (24) or (26) and (24). The details are omitted due to space constraints, but can be found in [73]. As far as this case study is concerned, comments similar to the single–tone one still hold. However, an important remark is worth being made to further emphasize, especially in this scenario, the robustness of the $\mathrm{T_c}$–DTR scheme with respect to other receivers. In the comments above, we have noticed that T_r and T_b might be optimized to reduce the effect of NBI in I_i for TR and DTR receivers, respectively. A similar optimization condition could be derived also for multi–tone interference. For example, with analytical steps similar to those in Section IV-A we would have $\sum_{k=1}^{N_I} J_k \mathrm{E}\left\{\alpha_{J_k}^2\right\} \cos(2\pi f_{J_k} T_X) = 0$ with $T_X = T_r$ and $T_X = T_b$ for TR and DTR receivers, respectively. Since, similar to $\mathrm{C_2}$ in (28) this is an optimization criterion that can be satisfied only on average, the optimization will have only a statistical meaning: this has a tremendous impact on the capability to reject the NBI. As a matter of fact, there will always be, instantaneously, a residual contribution in I_i, which will not allow these receivers to get a substantial performance improvement. On the other hand, it is worth mentioning that the statistical optimization criterion of $\mathrm{C_2}$ in (28) is much less sensitive to this problem because similar instantaneous fluctuations of channel fading in, *e.g.*, the numerator and the denominator of $\gamma_i(\cdot,\cdot;\cdot)$ in (14) have a different effect on the system performance: small fluctuations in the numerator have a much more pronounced effect. The interested reader can find further details and simulations about this point in [73, pp. 155–165, Sec. 5.6.4].

Eventually, we close this section with a comment about the computational complexity of all the receiver schemes studied and compared in this paper. It is important to note that all the detectors have the same decoding complexity. As a matter of fact, detection encompasses the same operations for all the receivers: i) multiplication of the received signal with a delayed version (the delay can be zero) of itself; ii) integration of a weighted version of the resulting energy signal; and iii) threshold comparison for data detection or timing acquisition. In fact, it is important to emphasize that the optimization criteria discussed in Section V and Section VI, are all performed off–line, *i.e.*, during the training or setup phase. Thus, no additional complexity is added during normal operation, *i.e.*, for data detection. So, since the decoding complexity is almost the same, we avoid to perform a precise complexity analysis in this paper. Of course, as mentioned in Section I, the receivers studied in this paper need a different number of delay lines and, thus, from the implementation point of view, differences among the receivers exist. In Section VII, we show, with some numerical examples, that there is a trade–off between architectural complexity and robustness to jamming.

VII. Numerical Results

This section shows some numerical examples to substantiate our analytical findings and claims.

a) System Setup: The following system setup is considered, unless otherwise stated, in what follows. i) The bandwidth (computed at -10dB with respect to the peak) of the transmitted pulse, $w(\cdot)$, is $B_w = 1.1\mathrm{GHz}$, ii) $T_c = 60\mathrm{ns}$, iii) $N_s = 32$, iv) the channel is assumed to be dense with $L = 10$, $T_w = 5\mathrm{ns}$, and no intra–pulse interference is considered, v) the multipath gains are Nakagami–m distributed with fading severity index $m = 2.5$, average power $\mathrm{E}\left\{\alpha_l^2\right\} = \mathrm{E}\left\{\alpha_0^2\right\}\exp(-\varepsilon l)$ for $l = 0, 1, \ldots, L-1$, and are normalized such that $\sum_{l=0}^{L-1} \mathrm{E}\left\{\alpha_l^2\right\} = 1$ with $\varepsilon = 0.45$[8], vi) $T_I = 20\mathrm{ns}$, which yields $L_{\mathrm{cap}} = 4$, vii) $f_{J_1} = 1\mathrm{GHz}$ for the single–tone scenario, which is approximately located around the peak of the pulse spectrum, viii) $f_{J_1} = 0.9054\mathrm{GHz}$ (GSM band)[9], $f_{J_2} = 1.38105\mathrm{GHz}$ (GNSS band), and $f_{J_3} = 2.452\mathrm{GHz}$ (802.11b Wi–Fi band) for the multi–tone scenario with $N_I = 3$, ix) $\{\alpha_{J_k}\}_{k=1}^{N_I}$ are assumed to be Rayleigh distributed with $\left\{\mathrm{E}\left\{\alpha_{J_k}^2\right\}\right\}_{k=1}^{N_I} = 1$, x) the decision threshold D_{th} is set according to a Constant False Alarm Rate (CFAR) optimization criterion [29] with $\mathrm{P_{fa}} = 10^{-3}$, xi) in the multi–tone scenario the jammers are assumed to be independent and identically distributed, and, in particular, the average powers $\{J_k\}_{k=1}^{N_I} = J_0$ take the same value, and xii) the SIR is defined as $\mathrm{SIR} = (N_s E_w)/(J_0 N_s T_X)$, with $T_X = T_c$ for $\mathrm{T_c}$–DTR, DTR, ED, CM–TR, and $T_X = 2T_r$ for TR. Furthermore, as far the optimization of the $\mathrm{T_c}$–DTR receiver is concerned, we adopt the following methodology. In a single–tone scenario, we first optimize T_c in (27) such that the condition $\cos(4\pi f_{J_k} T_c) = 1$ is verified, and then compute the optimal code such that the condition $\sum_{j=1}^{N_s-1} c_j c_{j-1} = -N_s$ is closely approached. In

[8]Although this channel model might be simple if compared to the recently standardized IEEE 802.15.4a channel model [9], it does not yield any limitations on either the generality of the conclusions drawn in this manuscript or the relative comparison among the different receiver architectures studied in this paper. Moreover, a similar channel model has been used in other papers available in the literature, *e.g.*, [38], because it might be seen as a simplified version of the channel model developed in [75] for the low frequency range, which has also been included in [9]. A recent study of the performance of a post–detection–integration receiver scheme over the IEEE 802.15.4a channel model with intentional jammers can be found in [76].

[9]GSM = Global System for Mobile communications. GNSS = Global Navigation Satellite Systems. Wi–Fi = Wireless Fidelity.

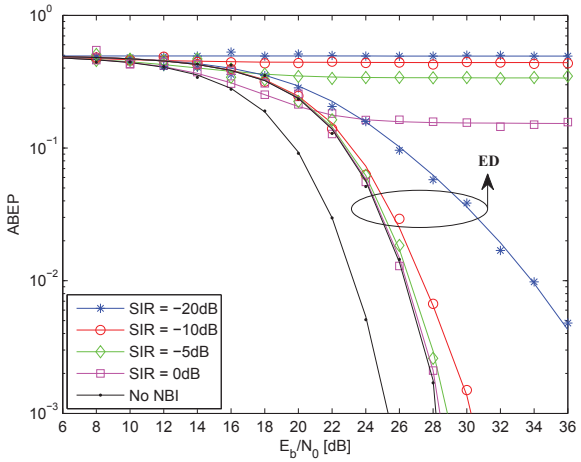

Fig. 2. ABEP of DTR and ED receivers. Solid lines: analytical model. Markers: Monte Carlo simulation. Parameter setup for DTR: i) BPAM modulation, ii) $T_c = 60$ns, and iii) $T_b = N_s T_c$. Parameter setup for ED: i) (Binary)PPM modulation, ii) $T_c = 120$ns, and iii) the PPM modulation shift is 60ns.

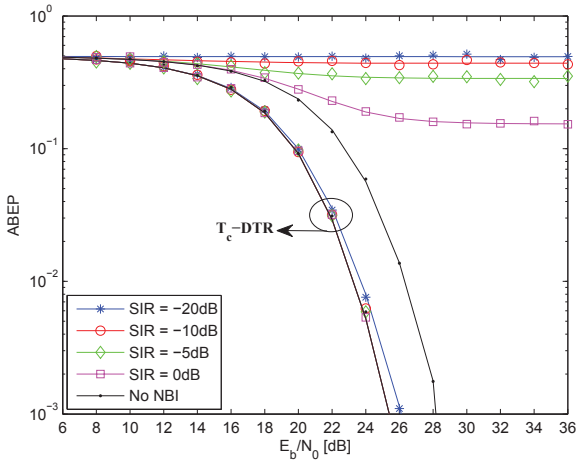

Fig. 3. ABEP of $\mathrm{T_c}$–DTR and TR receivers. Solid lines: analytical model. Markers: Monte Carlo simulation. As far as the $\mathrm{T_c}$–DTR scheme is considered, the optimal DS code design to meet the conditions C_1 and C_2 is considered. The used code is $[-1, +1, -1, +1, \ldots]$. Parameter setup for TR: i) BPAM modulation, and ii) $T_r = 60$ns.

a multi–tone scenario, owing to the system setup above, we use a similar methodology: first, T_c is chosen such that the condition $\sum_{k=1}^{N_I} \cos\left(4\pi f_{J_k} T_c\right) = N_I$ is closely satisfied, and then, similar to the single–tone scenario, the optimal code is computed such that the condition $\sum_{j=1}^{N_s-1} c_j c_{j-1} = -N_s$ is closely approached. The rest of the parameters can be found in the captions of each figure.

b) Single–Tone NBI – ABEP: In Figs. 2–4, we compare the performance of $\mathrm{T_c}$–DTR, TR, DTR, ED, and CM–TR receivers. In particular, the ABEP of the $\mathrm{T_c}$–DTR scheme is obtained by following the design guidelines described in Section V: both C_1 and C_2 have been taken into account, and an optimal code has been used. We can observe a substantial performance gain offered by the $\mathrm{T_c}$–DTR scheme. Note that

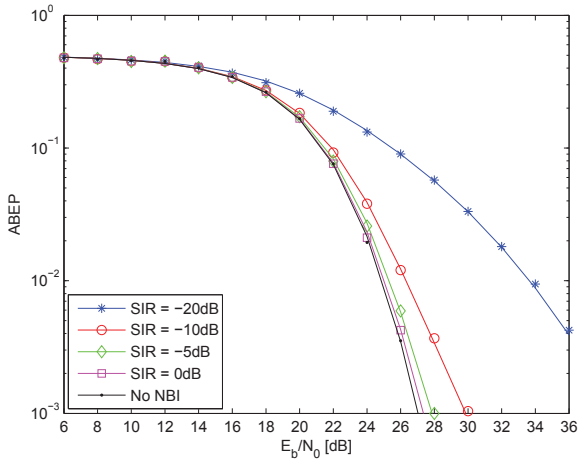

Fig. 4. ABEP of CM–TR receiver. Solid lines: analytical model. Markers: Monte Carlo simulation. Parameter setup: i) BPAM modulation, ii) $T_c = 60$ns, and iii) $T_b = N_s T_c$. Furthermore, the multiplexing codes are assumed to satisfy the condition in [12, Eq. (8)].

the performance of TR and DTR receivers is obtained without optimizing T_r and T_b to cancel out the interference contribution, I_i, in Table I. As a matter of fact, in this case the ABEP would be similar to that offered by the ED and the CM–TR schemes in Fig. 2 and in Fig. 4, respectively, with respect to which the $\mathrm{T_c}$–DTR scheme still performs much better.

In Figs. 5, 6, we analyze the performance offered by the $\mathrm{T_c}$–DTR scheme when code sequences typically adopted in the Spread Spectrum (SS) context are used. In particular, Walsh–Hadamard and Maximal–Length (ML) codes are considered [77]. A similar performance study for Gold and Kasami codes [77] can be found in [73], [78]. The ABEP for these codes is similar to that for ML codes. All DS codes have been selected among the different families in order to closely meet the conditions C_1 and C_2 in (27). We notice that except Walsh–Hadamard codes, which perfectly satisfy C_1 and closely approach C_2, the other codes are sub–optimal and show a significant error floor for strong NBI (low SIRs). This is mainly due to C_1 that is not satisfied. In particular, while for Walsh–Hadamard codes the performance gain offered by the $\mathrm{T_c}$–DTR scheme is significant and increases with the power of the interferer, when C_1 is not satisfied the $\mathrm{T_c}$–DTR solution can be worse than the ED or the CM–TR receivers. These results clearly show the importance of taking into account C_1 for a significant performance improvement. This is an important result for a multi–tone system setup: in Section V we have emphasized that C_2 can be optimized only on average. So, even though the optimization is only true in a statistical sense, the results in Figs. 5, 6 highlight that it can be good enough for a significant performance improvement. A careful analysis of the properties of Walsh–Hadamard codes for the optimization of the performance of the $\mathrm{T_c}$–DTR scheme can be found in [73, Table 5.4].

Moving from the results in Figs. 5, 6, in Fig. 7 we analyze the ABEP when C_2 is not optimized. As described in Section V, we notice that the $\mathrm{T_c}$–DTR scheme can never perform

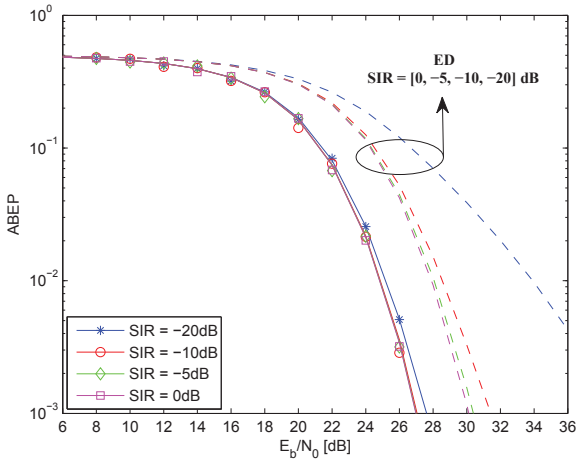

Fig. 5. ABEP of $\mathrm{T_c}$–DTR and ED receivers. Solid lines: analytical model. Markers: Monte Carlo simulation. As far as the $\mathrm{T_c}$–DTR scheme is considered, a Walsh–Hadamard code [77] with $N_s = 64$ is considered. The ED receiver for $N_s = 64$ is shown with dashed lines (only model).

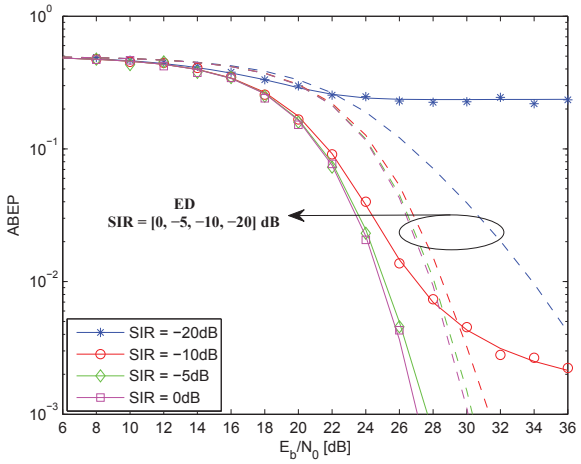

Fig. 6. ABEP of $\mathrm{T_c}$–DTR and ED receivers. Solid lines: analytical model. Markers: Monte Carlo simulation. As far as the $\mathrm{T_c}$–DTR scheme is considered, a ML code [77] with $N_s = 63$ is considered. The ED receiver for $N_s = 63$ is shown with dashed lines (only model).

worse than the ED or the CM–TR receivers.

Finally, we observe a very good agreement between Monte Carlo simulations and the analytical model developed in this paper. Moreover, the theoretical findings in Section V are well substantiated by the numerical results.

c) Single–Tone NBI – Miss Probability ($\mathrm{P_m} = 1 - \mathrm{P_d}$): In Figs. 8, 9, we show the Miss Probability, $\mathrm{P_m} = 1 - \mathrm{P_d}$. In particular, we can observe that also in this case the $\mathrm{T_c}$–DTR receiver offers an intrinsic robustness to strong NBI, while the rest of the receiver architectures exhibit a significant performance worsening for low SIRs. The curves for the CM–TR receiver are not shown because $\mathrm{T_c}$–DTR and CM–TR have similar trends for both ABEP and $\mathrm{P_m}$ (see Table I and Table II), and $\mathrm{T_c}$–DTR always outperforms CM–TR. Unlike the performance study of the ABEP conducted above, we can observe that in this case the worst receiver architecture

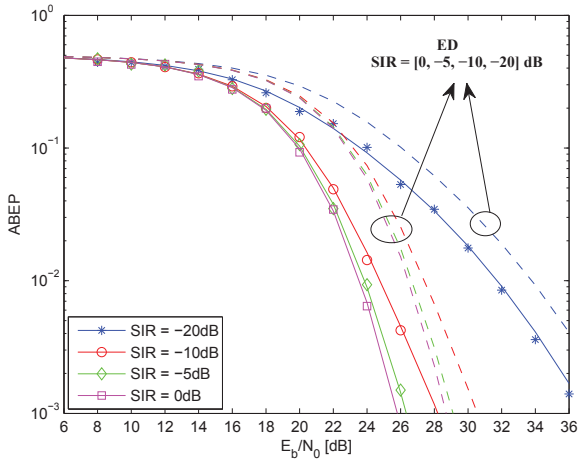

Fig. 7. ABEP of $\mathrm{T_c}$–DTR receiver when C_1 is verified and C_2 is not, *i.e.*, $\mathrm{C}_1 = 0$ and $\sum_{j=1}^{N_s-1} c_j c_{j-1} = +8$. Solid lines: analytical model. Markers: Monte Carlo simulation. The ED receiver is shown with dashed lines (only model).

is the ED, while both TR and DTR schemes do not show any floor thanks to the adaptive and optimized (*i.e.*, $I_i = 0$) design of T_r and T_c, respectively. As mentioned in Section V and Section VI, the condition $I_i = 0$ for TR and DTR receivers is equivalent to [74, Eq. (35)] when the AWGN is neglected. Thus, the results in Figs. 8, 9 might be thought as representative of the optimization strategy introduced in [74] as well. Furthermore, the absence of error floor on the curves confirm the conclusions drawn in [74]. As anticipated in Table II, the $\mathrm{T_c}$–DTR receiver exhibits a small performance degradation only for low SIRs: this stems from the impossibility to reduce to zero the effect of the NBI in $\mathrm{E}\left\{N_i^2\right\}$, as well as to completely cancel out I_i. Finally, we observe a very good agreement between Monte Carlo simulations and the analytical model developed in this paper. Also in this case, the theoretical findings in Section V are well substantiated by the numerical results.

d) Multi–Tone NBI – ABEP: In Figs. 10, 11, the ABEP of $\mathrm{T_c}$–DTR and ED receivers is shown, as a case study, for a multi–tone reference scenario, respectively. Among the various non–coherent receiver schemes already analyzed for the single–tone scenario, we have decided to focus our attention on the ED scheme because, along with the CM–TR detector, it is the best among the various solutions already available in the literature[10] (*i.e.*, the NBI has a less pronounced impact in the numerator of $\gamma_i(\cdot,\cdot;\cdot)$ in Table I). In fact, by using the approximation method in Section IV-A, we have $I_i \cong 0$ for both receivers, as described in Section V. On the other hand, the need to resort, in practice, to the optimization criterion in (28), which is true only statistically, does not make TR and DTR competitive with $\mathrm{T_c}$–DTR, ED, and CM–TR schemes. Numerical results substantiating this claim can be found in

[10]Note that, for the same SIR, ED and CM–TR have the same ABEP for low SIRs (see Table I). As a matter of fact, in this case the average power of each interferer for the CM–TR is twice that for the ED, due to the different chip times. However, the CM–TR receiver has a double data rate.

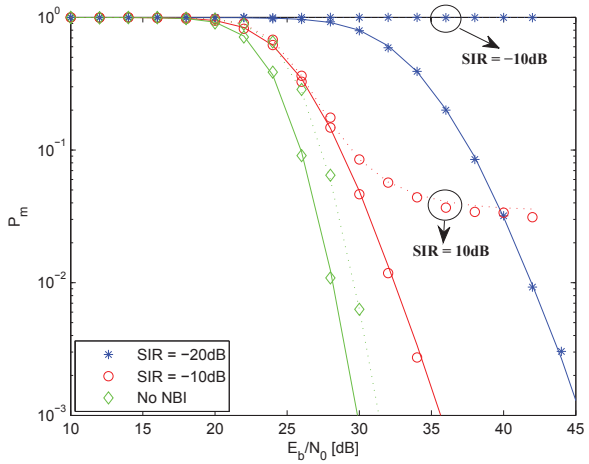

Fig. 8. $\mathrm{P_m}$ of DTR (solid lines with markers) and ED (dotted lines with markers) receivers. $T_c = T_b/N_s = 60.0078\mathrm{ns}$ and $T_c = 60\mathrm{ns}$ for DTR and ED receivers, respectively. For a fair comparison among the receivers, when possible, the parameters of each of them are chosen to optimize the performance. In detail, as far as the $\mathrm{T_c}$–DTR scheme is considered, the optimal DS code design to meet the conditions C_1 and C_2 is considered. The used code is $[-1,+1,-1,+1,\ldots]$. Moreover, $T_c = T_b/N_s = 60.0078\mathrm{ns}$ is chosen to closely approximate the condition $I_i = 0$ for the DTR receiver.

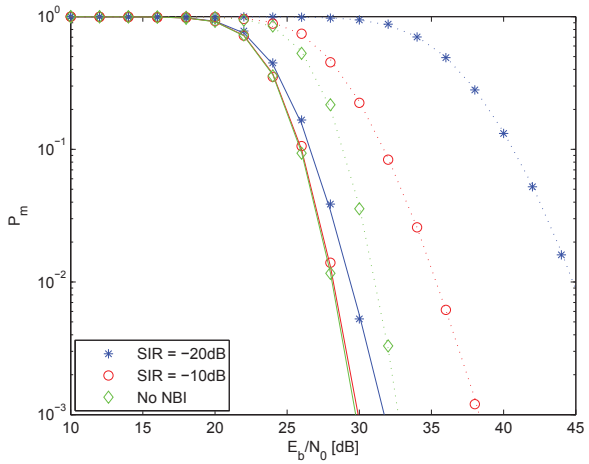

Fig. 9. $\mathrm{P_m}$ of $\mathrm{T_c}$–DTR (solid lines with markers) and TR (dotted lines with markers) receivers. $T_r = 60.25\mathrm{ns}$ for the TR receiver. For a fair comparison among the receivers, the parameters of each of them are chosen to optimize the performance. In detail, as far as the $\mathrm{T_c}$–DTR scheme is considered, the optimal DS code design to meet the conditions C_1 and C_2 is considered. The used code is $[-1,+1,-1,+1,\ldots]$. Moreover, $T_r = 60.25\mathrm{ns}$ is chosen to closely approximate the condition $I_i = 0$ for the TR receiver.

[73, pp, 190–191, Figs. 6.2–6.4], but are not reproduced here due to space constraints.

By comparing Fig. 10 and Fig. 11, we observe that also for multi–tone interference the $\mathrm{T_c}$–DTR scheme provides a substantial performance gain with respect to the ED. In particular, as long as $\mathrm{SIR} > -10\mathrm{dB}$, the aggregate NBI interference only slightly worsens the ABEP. As far as the accuracy of the analytical model in Section IV is concerned, interesting comments can be made. In Fig. 10, we notice that the simple approximation method in Section IV-A fails to be accurate

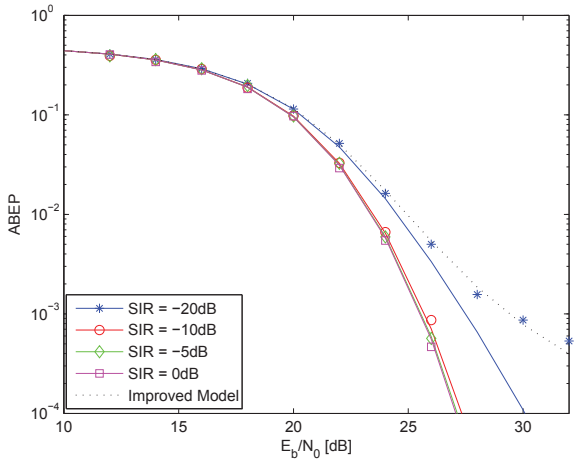

Fig. 10. ABEP of the $\mathrm{T_c}$–DTR receiver with 3 interferers located at $f_{J_1} = 0.9054\mathrm{GHz}$ (GSM band), $f_{J_2} = 1.38105\mathrm{GHz}$ (GNSS band), and $f_{J_3} = 2.452\mathrm{GHz}$ (802.11b Wi–Fi band). The "Improved Model" is given in Section IV-B. The receiver is optimized (on average) to reject the aggregate NBI (see (28)): i) $\mathrm{C}_1 = 0$, ii) $\sum_{j=1}^{N_s-1} c_j c_{j-1} = -31$, and iii) $T_c = 75.65\mathrm{ns}$.

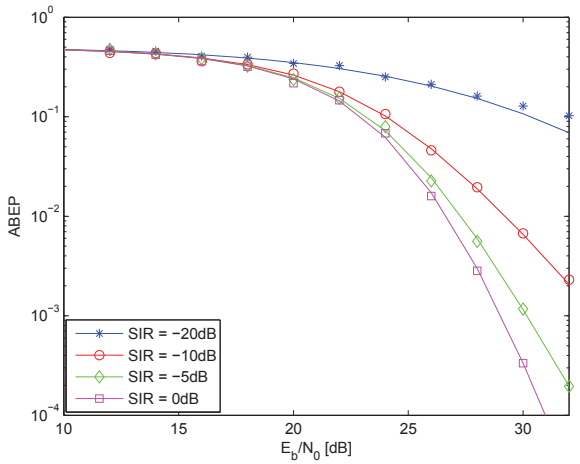

Fig. 11. ABEP of the ED receiver with 3 interferers located at $f_{J_1} = 0.9054\mathrm{GHz}$ (GSM band), $f_{J_2} = 1.38105\mathrm{GHz}$ (GNSS band), and $f_{J_3} = 2.452\mathrm{GHz}$ (802.11b Wi–Fi band). $T_c = 60\mathrm{ns}$

for very low SIRs (*i.e.*, $\mathrm{SIR} \leq -20\mathrm{dB}$ for each jammer), and the model under–estimates the ABEP. We have observed this trend for other system setups as well. On the other hand, the more complicated framework in Section IV-B is more accurate and well follows the results obtained with Monte Carlo simulations. This means that the optimization criterion used to obtain Fig. 10, which is based on the framework in Section IV-A, is sub–optimal and further improvements can be expected by using the more complicated optimization conditions coming from the framework in Section IV-B. A similar trend is observed in Fig. 11 for the ED receiver. In this case the framework in Section IV-A has always been used, and we can notice the better accuracy offered by it for $\mathrm{SIR} = -20\mathrm{dB}$ as well. However, some inaccuracies are well visible for high SNRs: beyond the point shown in the figure

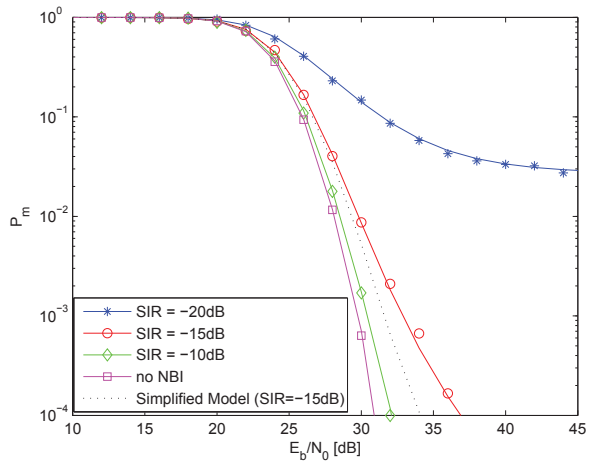

Fig. 12. $\mathrm{P_m}$ of the $\mathrm{T_c}$–DTR receiver with 3 interferers located at $f_{J_1} = 0.9054\mathrm{GHz}$ (GSM band), $f_{J_2} = 1.38105\mathrm{GHz}$ (GNSS band), and $f_{J_3} = 2.452\mathrm{GHz}$ (802.11b Wi–Fi band). The "Simplified Model" is that developed in Section IV-A. The receiver is optimized (on average) to reject the aggregate NBI (see (28)): i) $\mathrm{C}_1 = 0$, ii) $\sum_{j=1}^{N_s-1} c_j c_{j-1} = -31$, and iii) $T_c = 75.65\mathrm{ns}$. Moreover, pulse shaping is also adopted to reject the jamming frequency f_{J_1} (see Appendix I), which is located around the peak of the pulse's spectrum.

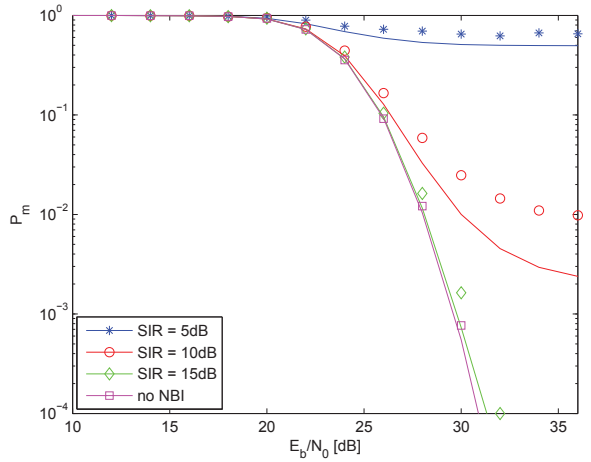

Fig. 13. $\mathrm{P_m}$ of the DTR receiver with 3 interferers located at $f_{J_1} = 0.9054\mathrm{GHz}$ (GSM band), $f_{J_2} = 1.38105\mathrm{GHz}$ (GNSS band), and $f_{J_3} = 2.452\mathrm{GHz}$ (802.11b Wi–Fi band). The receiver is optimized (on average) to reject the aggregate NBI, *i.e.*, $T_c = 87.90\mathrm{ns}$.

the framework starts being less accurate and under–estimates the ABEP. In summary, both frameworks in Section IV can be used for adequate SIRs with a reasonable accuracy, in spite of their simplicity (especially the framework in Section IV-A).

e) Multi–Tone NBI – Miss Probability ($\mathrm{P_m} = 1 - \mathrm{P_d}$)*:* In Figs. 12, 13, the $\mathrm{P_m}$ of $\mathrm{T_c}$–DTR and DTR receivers is shown, respectively, for a multi–tone reference scenario. We can notice that, for the same requirement on the $\mathrm{P_{fa}}$, the receivers are not comparable to one another: the $\mathrm{T_c}$–DTR receiver is much better for higher jamming powers. The reason follows immediately from Section VI, where it is shown that the DTR scheme can satisfy the condition $I_i \cong 0$ only on average, while for the $\mathrm{T_c}$–DTR scheme it is sufficient to use a balanced code to meet this requirement for a large set of SIRs (see Section IV-A). For very low SIRs, the framework in Section IV-B should be used and the balanced code design would no longer be optimal.

Let us now carefully analyze Figs. 12, 13 from the point of view of the approximation accuracy of the analytical frameworks described in Section IV. From Fig. 12, we notice that the framework in Section IV-A, when used for computing $\mathrm{P_m}$, seems to be less accurate than when used for computing the ABEP in Fig. 10. We notice that it starts under–estimating the actual $\mathrm{P_m}$ for $\mathrm{SIR} = -15\mathrm{dB}$. For this reason in Fig. 12 the model in Section IV-B is used for all curves. Both frameworks in Section IV yield the same accuracy for $\mathrm{SIR} > -15\mathrm{dB}$. In Fig. 13, we have deliberately used only the framework developed in Section IV-A in order to clearly show that for low SIRs the interfering signals at the detector input cannot be actually summed up in power. The framework in Section IV-A starts under–estimating the $\mathrm{P_m}$ for $\mathrm{SIR} < 10\mathrm{dB}$. However, even though a few dB of error can be observed, the framework is still able to capture the error floor for all analyzed SIRs: this is important to qualitatively figure out the break–down point of this receiver, or, in other words, the point after which it can no longer be used in practice due its poor performance. Better approximations can be obtained by adopting the framework in Section IV-B, as already verified for the $\mathrm{T_c}$–DTR receiver.

VIII. Conclusion

In this paper, we have analyzed the performance of various low–complexity receiver schemes and shown, via analysis and simulation, the inherent robustness to NBI of the $\mathrm{T_c}$–DTR scheme. A simple but insightful analytical framework has been proposed and used for system optimization of this latter receiver. In particular, the optimal design of the DS code to cancel out the NBI for single– and multi–tone reference scenarios has been developed, and its efficiency has been substantiated for various system setups. Although we have also remarked that the simplest framework proposed in this paper could be inaccurate for some scenarios, we have highlighted that it can well capture the qualitative behavior of the system even for low SIRs. Furthermore, and more important, we have shown that it is insightful for understanding the reasons of the improved performance and robustness to NBI offered by the $\mathrm{T_c}$–DTR scheme with respect to other non–coherent solutions. Finally, our empirical trials have shown that this simple framework is an actual lower–bound of both ABEP and $\mathrm{P_m}$ of $\mathrm{T_c}$–DTR receivers. In summary, analysis and simulation have substantiated that an optimized $\mathrm{T_c}$–DTR receiver can outperform of several dB other well–known non–coherent schemes operating in the same environment.

Appendix I
Computation of U_i, I_i, $\tilde{N}_i$ in (13)

Let us consider, without loss of generality, the transmitted bit with index $i = \lfloor j/N_s \rfloor = 0$ for $j = 0, 1, \ldots, N_s - 1$, *i.e.*, $b_i = b_0$. The decision variable $Q_i = Q_0$ in (8) can be written as shown in (29) on top of this page, where we have

$$\begin{aligned} Q_0 = & \sum_{j=0}^{N_s-1}\left[\int_0^{T_I} b_0\psi^2(t)\,dt\right] + \sum_{j=0}^{N_s-1}\left[\int_0^{T_I} b_0\tilde{c}_j\psi(t)\left(\xi_{\Delta,j}(t)+\eta_{\Delta,j}(t)\right)dt\right] \\ & + \sum_{j=0}^{N_s-1}\left[\int_0^{T_I} b_0\tilde{c}_{j-1}\psi(t)\left(\xi_j(t)+\eta_j(t)\right)dt\right] + \sum_{j=0}^{N_s-1}\left[\int_0^{T_I} c_j\left(\xi_j(t)+\eta_j(t)\right)\left(\xi_{\Delta,j}(t)+\eta_{\Delta,j}(t)\right)dt\right] \end{aligned} \tag{29}$$

$$\begin{cases} U_0 = \displaystyle\sum_{j=0}^{N_s-1}\left[\int_0^{T_I} b_0\psi^2(t)\,dt\right] = b_0 N_s E_w \sum_{l=0}^{L_{\mathrm{CAP}}-1}\alpha_l^2 \\ I_0^{(1)} = \displaystyle\sum_{j=0}^{N_s-1}\left[\int_0^{T_I} b_0\tilde{c}_j\psi(t)\,\xi_{\Delta,j}(t)\,dt\right] \overset{(a)}{=} \sqrt{2J_1}\sqrt{E_w}\,|W(f_{J_1})|\,\alpha_{J_1}\displaystyle\sum_{j=0}^{N_s-1}\sum_{l=0}^{L_{\mathrm{CAP}}-1}\left[\tilde{c}_j\alpha_l\cos\left(\Psi_{l,j}-2\pi f_{J_1}T_c\right)\right] \\ I_0^{(2)} = \displaystyle\sum_{j=0}^{N_s-1}\left[\int_0^{T_I} b_0\tilde{c}_{j-1}\psi(t)\,\xi_j(t)\,dt\right] \overset{(b)}{=} \sqrt{2J_1}\sqrt{E_w}\,|W(f_{J_1})|\,\alpha_{J_1}\displaystyle\sum_{j=0}^{N_s-1}\sum_{l=0}^{L_{\mathrm{CAP}}-1}\left[\tilde{c}_{j-1}\alpha_l\cos\left(\Psi_{l,j}\right)\right] \\ I_0^{(3)} = \displaystyle\sum_{j=0}^{N_s-1}\left[\int_0^{T_I} c_j\xi_j(t)\,\xi_{\Delta,j}(t)\,dt\right] \overset{(c)}{\approx} J_1 T_I\alpha_{J_1}^2\cos\left(2\pi f_{J_1}T_c\right)\displaystyle\sum_{j=0}^{N_s-1}c_j \end{cases} \tag{30}$$

$$\begin{aligned} \tilde{N}_0 = & \underbrace{\sum_{j=0}^{N_s-1}\left[\int_0^{T_I} b_0\tilde{c}_{j-1}\psi(t)\,\eta_j(t)\,dt\right]}_{\mathrm{N_A}} + \underbrace{\sum_{j=0}^{N_s-1}\left[\int_0^{T_I} b_0\tilde{c}_j\psi(t)\,\eta_{\Delta,j}(t)\,dt\right]}_{\mathrm{N_B}} + \underbrace{\sum_{j=0}^{N_s-1}\left[\int_0^{T_I} c_j\xi_j(t)\,\eta_{\Delta,j}(t)\,dt\right]}_{\mathrm{N_C}} \\ & + \underbrace{\sum_{j=0}^{N_s-1}\left[\int_0^{T_I} c_j\xi_{\Delta,j}(t)\,\eta_j(t)\,dt\right]}_{\mathrm{N_D}} + \underbrace{\sum_{j=0}^{N_s-1}\left[\int_0^{T_I} c_j\eta_j(t)\,\eta_{\Delta,j}(t)\,dt\right]}_{\mathrm{N_E}} \end{aligned} \tag{31}$$

defined $\psi(t) = (w\otimes h)(t)$, $\eta_j(t) = \tilde{n}(t+jT_c)$, $\xi_j(t) = J(t+jT_c)$, $\eta_{\Delta,j}(t) = \eta_j(t-T_c)$, and $\xi_{\Delta,j}(t) = \xi_j(t-T_c)$.

By using the channel model in Section II-B, the noise–less terms are shown in (30) on top of this page, where we have defined $\Psi_{l,j} = 2\pi f_{J_1}(lT_w + jT_c) + \theta_{J_1} - \arg\{W(f_{J_1})\}$, $k = \sqrt{-1}$ is the imaginary unit, $|\cdot|$ and $\arg\{\cdot\}$ denote the modulus and the phase of a complex number, respectively, and $W(f) = \int_{-\infty}^{+\infty} w(t)\exp(-2\pi kft)\,dt = |W(f)|\exp(\arg\{W(f)\})$ is the Fourier transform of $w(\cdot)$.

In particular, (30) is obtained by using a procedure similar to [38]: $\overset{(a)}{=}$ and $\overset{(b)}{=}$ are computed by exploiting the Parseval's theorem, and $\overset{(c)}{\approx}$ by taking into account that for typical setups we have $T_I \gg (4\pi f_{J_1})^{-1}$. Furthermore, the condition $I_0^{(1)} + I_0^{(2)} \ll U_0 + I_0^{(3)}$ follows immediately from the out–of–phase summation of various terms in $I_0^{(1)}$ and $I_0^{(2)}$, along with the pseudo–random properties of typical DS codes and their differentially encoded version. In addition, both terms could be made arbitrarily small via a proper shaping of the transmitted pulse, *i.e.*, by designing the transmitted pulse such that the condition $|W(f_{J_1})| = 0$ is satisfied.

Let us now consider the noisy terms of Q_0 in (29). They are shown in (31) on top of this page. From (31), the noise power, $\mathrm{E}\left\{\tilde{N}_0^2\right\}$, can be written as follows:

$$\begin{aligned} \mathrm{E}\left\{\tilde{N}_0^2\right\} = & \mathrm{E}\left\{\tilde{\mathrm{N}}_\alpha^2\right\} + \mathrm{E}\left\{\tilde{\mathrm{N}}_\beta^2\right\} + \mathrm{E}\left\{\tilde{\mathrm{N}}_\gamma^2\right\} \\ & + 2\mathrm{E}\left\{\tilde{\mathrm{N}}_\alpha\tilde{\mathrm{N}}_\beta\right\} + 2\mathrm{E}\left\{\tilde{\mathrm{N}}_\alpha\tilde{\mathrm{N}}_\gamma\right\} + 2\mathrm{E}\left\{\tilde{\mathrm{N}}_\beta\tilde{\mathrm{N}}_\gamma\right\} \end{aligned} \tag{32}$$

where we have defined $\tilde{\mathrm{N}}_\alpha = \mathrm{N_A} + \mathrm{N_B}$, $\tilde{\mathrm{N}}_\beta = \mathrm{N_C} + \mathrm{N_D}$, and $\tilde{\mathrm{N}}_\gamma = \mathrm{N_E}$.

By using arguments similar to [5], [29], [71], the following identities and approximations can be proved after lengthly algebraic manipulations:

$$\begin{cases} \mathrm{E}\left\{\tilde{\mathrm{N}}_\alpha^2\right\} = (2N_s-1)N_0E_w\displaystyle\sum_{l=0}^{L_{\mathrm{CAP}}-1}\alpha_l^2 \\ \mathrm{E}\left\{\tilde{\mathrm{N}}_\beta^2\right\} \overset{(d)}{\approx} J_1T_IN_0\alpha_{J_1}^2\left[N_s + \displaystyle\sum_{j=1}^{N_s-1}c_jc_{j-1}\cos\left(4\pi f_{J_1}T_c\right)\right] \\ \mathrm{E}\left\{\tilde{\mathrm{N}}_\gamma^2\right\} \approx 0.5N_0^2N_sWT_I \\ \mathrm{E}\left\{\tilde{\mathrm{N}}_\alpha\tilde{\mathrm{N}}_\beta\right\} \overset{(e)}{\approx} 0 \\ \mathrm{E}\left\{\tilde{\mathrm{N}}_\alpha\tilde{\mathrm{N}}_\gamma\right\} = E\left\{\tilde{\mathrm{N}}_\beta\tilde{\mathrm{N}}_\gamma\right\} = 0 \end{cases} \tag{33}$$

In particular: i) $\overset{(d)}{\approx}$ is valid under the assumption $T_I \gg$

$(4\pi f_{J_1})^{-1}$, and ii) $\overset{(e)}{\approx}$ can be obtained by following the same arguments as those exploited to get $\overset{(a)}{=}$ and $\overset{(b)}{=}$ in (30), and by relying on the pseudo–random properties of the DS code as well. Exact expressions similar to $\overset{(a)}{=}$ and $\overset{(b)}{=}$ could be easily derived, but are here omitted due to space constraints.

REFERENCES

[1] C. K. Rushforth, "Transmitted-reference techniques for random or unknown channels", *IEEE Trans. Inform. Theory*, vol. 10, no. 1, pp. 39-42, Jan. 1964.

[2] R. Gagliardi, "A geometrical study of transmitted reference communication system", *IEEE Trans. Commun.*, vol. 12, no. 4, pp. 118-123, Dec. 1964.

[3] R. Hoctor and H. Tomlinson, "Delay–hopped transmitted–reference RF communications", *IEEE Conf. Ultra–Wideband Systems and Technologies*, pp. 265-269, May 2002.

[4] M. Ho, V. S. Somayazulu, J. Foerster, and S. Roy, "A differential detector for an ultra–wideband communications system", *IEEE Vehic. Technol. Conf. – Spring*, vol. 4, pp. 1896–1900, May 2002.

[5] J. D. Choi and W. E. Stark, "Performance of ultra–wideband communications with suboptimal receivers in multipath channels", *IEEE J. Sel. Areas Commun.*, vol. 20, no. 9, pp. 1754–1766, Dec. 2002.

[6] K. Witrisal *et al.*, "Noncoherent ultra–wideband systems", *IEEE Sig. Process. Mag.*, vol. 26, no. 4, pp. 48–66, July 2009.

[7] M. Z. Win and R. A. Scholtz, "On the energy capture of ultrawide bandwidth signals in dense multipath environments", *IEEE Commun. Lett.*, vol. 2, no. 9, pp. 245–247, Sep. 1998.

[8] J. Karedal *et al.*, "A Measurement–based statistical model for industrial ultra–wideband channels", *IEEE Trans. Wireless Commun.*, vol. 6, no. 8, pp. 3028–3037, Aug. 2007.

[9] A. F. Molisch *et al.*, "A comprehensive standardized model for ultra-wideband propagation channels", *IEEE Trans. Antennas Prop.*, vol. 54, no. 11, pp. 3151–3166, Nov. 2006.

[10] M. Di Renzo *et al.*, "The ultra–wide bandwidth outdoor channel: From measurement campaign to statistical modelling", *Mobile Networking and Applications*, vol. 11, pp. 451–467, Aug. 2006.

[11] D. Goeckel and Q. Zhang, "Slightly frequency–shifted reference ultra–wideband (UWB) radio", *IEEE Trans. Commun.*, vol. 55, no. 3, pp. 508–519, Mar. 2007.

[12] A. D'Amico and U. Mengali, "Code–multiplexed UWB transmitted–reference radio", *IEEE Trans. Commun.*, vol. 56, no. 12, pp. 2125–2132, Dec. 2008.

[13] J. L. Paredes, G. R. Arce, and Z. Wang, "Ultra–wideband compressed sensing: Channel estimation", *IEEE J. Select. Topics Sign. Process.*, vol. 1, no. 3, pp. 383–395, Oct. 2007.

[14] P. Zhang, Z. Hu, R. C. Qiu, and B. M. Sadler, "A compressed sensing based ultra–wideband communication system", *IEEE Int. Conf. Commun.*, pp. 1–5, June 2009.

[15] J. Meng, J. Ahmadi–Shokouh, H. Li, E. J. Charlson, Z. Han, S. Noghanian, and E. Hossain, "Sampling rate reduction for 60 GHz UWB communication using compressive sensing", *Asilomar Conf. on Signals, Systems, and Computers*, pp. 1–5, Nov. 2009.

[16] A. Oka and L. Lampe, "A compressed sensing receiver for UWB impulse radio in bursty applications like wireless sensor networks", *Elsevier Physical Commun.*, vol. 2, no. 4, pp. 248–264, Dec. 2009.

[17] P. Zhang and R. C. Qiu, "Wireless tomography, part III: Compressed sensing for ultra–wideband signals", *Int. Waveform Diversity and Design Conf.*, pp. 1–6, Aug. 2010.

[18] L. Yang and G. B. Giannakis, "Timing ultra–wideband signals with dirty templates", *IEEE Trans. Commun.*, vol. 53, no. 11, pp. 1952–1963, Nov. 2005.

[19] A. D'Amico and L. Taponecco, "A differential receiver for UWB systems", *IEEE Trans. Wireless Commun.*, vol. 5, no. 7, pp. 1601–1605, July 2006.

[20] S. Zhao, H. Liu, and Z. Tian, "Decision directed autocorrelation receivers for pulsed ultra–wideband systems", *IEEE Trans. Wireless Commun.*, vol. 5, no. 8, pp. 2175–2184, Aug. 2006.

[21] C. Carbonelli and U. Mengali, "Noncoherent receivers for UWB applications", *IEEE Trans. Wireless Commun.*, vol. 5, no. 8, pp. 2285–2294, Aug. 2006.

[22] F. Tufvesson, S. Gezici, and A. F. Molisch, "Ultra–wideband communications using hybrid matched filter correlation receivers", *IEEE Trans. Wireless Commun.*, vol. 5, no. 11, pp. 3119–3129, Nov. 2006.

[23] A. D'Amico, U. Mengali, and E. Arias–de–Reyna, "Energy–detection UWB receivers with multiple energy measurements", *IEEE Trans. Wireless Commun.*, vol. 6, no. 7, pp. 2652–2659, July 2007.

[24] Q. H. Dang and A.–J. van der Veen, "A decorrelating multiuser receiver for transmit–reference UWB systems", *IEEE J. Select. Signal Process.*, vol. 1, no. 3, pp. 431–442, Oct. 2007.

[25] H. Xu and L. Yang, "Differential UWB communications with digital multicarrier modulation", *IEEE Trans. Signal Process.*, vol. 56, no. 1, pp. 284–295, Jan. 2008.

[26] Y. Chen and N. C. Beaulieu, "Improved receivers for generalized UWB transmitted reference systems", *IEEE Trans. Wireless Commun.*, vol. 7, no. 2, pp. 500–504, Feb. 2008.

[27] Tao Jia and D. I. Kim, "Multiple access performance of balanced UWB transmitted–reference systems in multipath", *IEEE Trans. Wireless Commun.*, vol. 7, no. 3, pp. 1084–1094, Mar. 2008.

[28] V. Lottici and Z. Tian, "Multiple symbol differential detection for UWB communications", *IEEE Trans. Wireless Commun.*, vol. 7, no. 5, pp. 1656–1666, May 2008.

[29] M. Di Renzo, L. A. Annoni, F. Graziosi, and F. Santucci, "A novel class of algorithms for timing acquisition of differential transmitted reference UWB receivers: Architecture, performance analysis and system design", *IEEE Trans. Wireless Commun.*, vol. 7, no. 6, pp. 2368–2387, June 2008.

[30] X. Dong, L. Jin, and P. Orlik, "A new transmitted reference pulse cluster system for UWB communications", *IEEE Trans. Vehic. Technol.*, vol. 57, no. 5, pp. 3217–3224, Sep. 2008.

[31] Q. Zhang and A. Nallanathan, "Transmitted–reference impulse radio systems based on selective combining", *IEEE Trans. Wireless Commun.*, vol. 7, no. 11, pp. 4105–4109, Nov. 2008.

[32] S. Gezici, "Coded–reference ultra–wideband systems", *IEEE Int. Conf. on Ultra–Wideband*, vol. 3, pp. 117–120, Sep. 2008.

[33] A. D'Amico and U. Mengali, "Multiuser UWB communication systems with code–multiplexed transmitted–reference", *IEEE Int. Commun. Conf.*, pp. 3765–3769, May 2008.

[34] M. Ouertani, X. Huilin, H. Besbes, L. Yang, and A. Bouallegue, "Differential (de)modulation for orthogonal bi–pulse noncoherent UWB", *IEEE Int. Commun. Conf.*, pp. 1–6, June 2009.

[35] J. Zhang and L. W. Hanlen, "Non–coherent receiver with fractional sampling for impulsive UWB systems", *IEEE Int. Commun. Conf.*, pp. 1–5, June 2009.

[36] Y.–L. Chao and R. A. Scholtz, "Ultra–wideband transmitted reference systems", *IEEE Trans. Vehic. Technol.*, vol. 54, no. 5, pp. 1556–1569, Sep. 2005.

[37] T. Q. S. Quek and M. Z. Win, "Analysis of UWB transmitted–reference communication systems in dense multipath channels", *IEEE J. Select. Areas Commun.*, vol. 23, no. 9, pp. 1863–1874, Sep. 2005.

[38] T. Q. S. Quek, M. Z. Win, and D. Dardari, "Unified analysis of UWB transmitted–reference schemes in the presence of narrowband interference", *IEEE Trans. Wireless Commun.*, vol. 6, no. 6 pp. 2126–2139, June 2007.

[39] A. Rabbachin *et al.*, "UWB energy detection in the presence of multiple narrowband interferers", *IEEE Int. Conf. on Ultra–Wideband*, pp. 857–862, Sep. 2007.

[40] Y. D. Alemseged and K. Witrisal, "Modeling and mitigation of narrowband interference for transmitted–reference UWB systems", *IEEE J. Select. Signal Process.*, vol. 1, no. 3, pp. 456–469, Oct. 2007.

[41] A. Rabbachin, "Low complexity UWB receivers with ranging capabilities", *Ph.D. Dissertation*, University of Oulu, May 2008.

[42] M. Di Renzo, F. Graziosi, and F. Santucci, "A framework for computing detection and false alarm probabilities for IR–UWB transmitted reference receivers over generalized fading channels with tone interference", *IEEE Int. Symp. Spread Spectrum Techniques and Applications*, pp. 297–302, Aug. 2008.

[43] L. Zhiguo, H. Joshi, D. Goeckel, D. Gupta, and A. Mathew, "Performance of UWB systems in the presence of severe multipath and narrowband interference", *IEEE Int. Conf. on Ultra–Wideband*, pp. 85–88, Sep. 2008.

[44] A. Rabbachin, T. Q. S. Quek, P. C. Pinto, I. Oppermann, and M. Z. Win, "Effect of aggregate narrowband interference on the UWB autocorrelation receiver", *IEEE Int. Conf. on Ultra–Wideband*, pp. 79–83, Sep. 2008.

[45] A. Rabbachin, T. Q. S. Quek, P. C. Pinto, I. Oppermann, and M. Z. Win, "Non–coherent UWB communications in the presence of multiple narrowband interferers", *IEEE Trans. Wireless Commun.*, vol. 9, no. 11, pp. 3365–3379, Nov. 2010.

[46] S. Niranjayan and N. Beaulieu, "General performance analysis of TR UWB systems", *IEEE Trans. Wireless Commun.*, vol. 7, no. 12, pp. 5268–5277, Dec. 2008.

[47] D. I. Kim, "Multiuser performance of M–ary orthogonal coded/balanced UWB transmitted–reference systems", *IEEE Trans. Commun.*, vol. 57, no. 4, pp. 1013–1024, Apr. 2009.
[48] K. Maichalernnukul, T. Kaiser, and F. Zheng, "On the performance of coherent and noncoherent UWB detection systems using a relay with multiple antennas", *IEEE Trans. Wireless Commun.*, vol. 8, no. 7, pp. 3407–3414, July 2009.
[49] M. Di Renzo, F. Graziosi, and F. Santucci, "On the cumulative distribution function of quadratic–form receivers over generalized fading channels with tone interference", *IEEE Trans. Commun.*, vol. 57, no. 7, pp. 2122–2137, July 2009.
[50] A. Rabbachin, T. Q. S. Quek, I. Oppermann, and M. Z. Win, "Effect of uncoordinated network interference on UWB autocorrelation receiver", *IEEE Int. Conf. on Ultra–Wideband*, Vancouver, Canada, Sep. 2009.
[51] A. Conti, D. Dardari, G. Pasolini, and O. Andrisano, "Bluetooth and IEEE 802.11b coexistence: Analytical performance evaluation in fading channels", *IEEE J. Sel. Areas Commun.*, vol. 21, no. 2, pp. 259–269, Feb. 2003.
[52] C. R. C. M. da Silva and L. B. Milsteinn, "Spectral–encoded UWB communication systems: Real–time implementation and interference suppression", *IEEE Trans. Commun.*, vol. 53, no. 8, pp. 1391–1401, Aug. 2005.
[53] A. Giorgetti, M. Chiani, and M. Z. Win, "The effect of narrowband interference on wideband wireless communication systems", *IEEE Trans. Commun.*, vol. 53, no. 12, pp. 2139–2149, Dec. 2005.
[54] C R. C. M. da Silva and L. B. Milstein, "The effects of narrowband interference on UWB communication systems with imperfect channel estimation", *IEEE J. Select. Areas Commun.*, vol. 24, no. 4, pp. 717–723, Apr. 2006.
[55] A. Giorgetti, M. Chiani, and D. Dardari, "Coexistence issues in cognitive radios based on ultra–wide bandwidth systems", *IEEE Int. Conf. on Cognitive Radio Oriented Wireless Net. and Commun.*, pp. 1–5, June 2006.
[56] M. Z. Win, P. C. Pinto, A. Giorgetti, M. Chiani, and L. Shepp, "Error performance of ultrawideband systems in a Poisson field of narrowband interferers", *IEEE Int. Symp. on Spread Spectrum Techniques and Applications*, pp. 28–31, Aug. 2006.
[57] B. Hu and N. C. Beaulieu, "Performance of an ultra–wideband communication system in the presence of narrowband BPSK– and QPSK–modulated OFDM interference", *IEEE Trans. Commun.*, vol. 54, no. 10, pp. 1720–1724, Oct. 2006.
[58] S. Kai, Z. Yi, B. Kelleci, T. W. Fischer, E. Serpedin, and A. I. Karsilayan, "Impacts of narrowband interference on OFDM–UWB receivers: analysis and mitigation", *IEEE Trans. Signal Process.*, vol. 55, no. 3, pp. 1118–1128, Mar. 2007.
[59] M. E. Sahin, S. Ahmed, and H. Arslan, "The roles of ultra wideband in cognitive networks", *IEEE Int. Conf. on Ultra–Wideband*, pp. 247–252, Sep. 2007.
[60] M. Chiani and A. Giorgetti, "Coexistence between UWB and narrow–band wireless communication systems", *Proc. of the IEEE*, vol. 97, no. 2, pp. 231–254, Feb. 2009.
[61] P. C. Pinto, A. Giorgetti, M. Z. Win, and M. Chiani, "A stochastic geometry approach to coexistence in heterogeneous wireless networks", *IEEE J. Sel. Areas Commun.*, vol. 27, no. 7, pp. 1268–1282, Sep. 2009.
[62] S. Colson and H. Hoff, "Ultra–wideband technology for defence applications", *IEEE Int. Conf. on Ultra–Wideband*, pp. 615–620, Sep. 2005.
[63] F. Dowla, F. Nekoogar, and A. Spiridon, "Interference mitigation in transmitted–reference ultra–wideband (UWB) receivers", *IEEE Int. Symp. on Antennas and Propagation*, vol. 2, pp. 1307–1310, June 2004.
[64] O. Ozdemir, Z. Sahinoglu, and J. Zhang, "Narrowband interference resilient receiver design for unknown UWB signal detection", *IEEE Int. Commun. Conf.*, pp. 785–789, May 2008.
[65] S. Cui, K. C. Teh, K. H. Li, Y. L. Guan, and C. L. Law, "Performance analysis of transmitted–reference UWB systems with narrowband interference suppression", *Wireless Communications and Mobile Computing*, July 2008.
[66] C. Steiner and A. Wittneben, "Cognitive interference suppression for low complexity UWB transceivers", *IEEE Int. Conf. on Ultra–Wideband*, pp. 165–168, Sep. 2008.
[67] D. Gupta, L. Zhiguo, and P. Kelly, "Interference detection and rejection in ultra–wideband systems", *IEEE Int. Conf. on Ultra–Wideband*, pp. 67–70, Sep. 2008.
[68] R. A. Scholtz, P. V. Kumar, and C. J. Corrada–Bravo, "Signal design for ultra–wideband radio", *Sequences and their Applications*, pp. 1–15, May 2001.
[69] M. Di Renzo, F. Graziosi, and F. Santucci, "A framework for the analysis of UWB receivers in sparse multipath channels with intra–pulse interference via Padé expansion", *IEEE Trans. Commun.*, vol. 56, no. 4, pp. 535–541, Apr. 2008.
[70] M. Di Renzo, D. De Leonardis, F. Graziosi, and F. Santucci, "Timing acquisition performance metrics of T_c–DTR UWB receivers over frequency–selective fading channels with narrow–band interference", *IEEE Military Commun. Conf.*, pp. 1–6, Oct. 2010.
[71] C. Yi–Ling and R. A. Scholtz, "Optimal and suboptimal receivers for ultra–wideband transmitted reference systems", *IEEE Global Telecommun. Conf.*, pp. 759–763, Dec. 2003.
[72] S. Verdu, *Multiuser Detection*, Cambridge University Press, Aug. 1998.
[73] D. De Leonardis, "Cognitive ultra wide–band: Design, performance analysis, and optimization of a low–complexity receiver robust to narrow–band interference", *Master Thesis*, University of L'Aquila, May 2009. Available upon request.
[74] M. Pausini and G. J. M. Janssen, "On the narrowband interference in transmitted reference UWB receivers", *IEEE Int. Conf. on Ultra–Wideband*, pp. 571–575, Sep. 2005.
[75] D. Cassioli, M. Z. Win, and A. F. Molisch, "The ultra–wide bandwidth indoor channel – From statistical model to simulations", *J. Select. Areas Commun.*, vol. 20, no. 6, pp. 1247–1257, Aug. 2002.
[76] M. Di Renzo, F. Tempesta, L. A. Annoni, F. Santucci, F. Graziosi, R. Minutolo, and M. Montanari, "Performance evaluation of IR–UWB D–Rake receivers over IEEE 802.15.4a multipath fading channels with narrow–band interference", *IEEE Int. Conf. on Ultra–Wideband*, pp. 71–76, Sep. 2009.
[77] M. K. Simon, J. Omura, R. Scholtz, and B. Levitt, *Spread Spectrum Communications Handbook*, McGraw–Hill, Sep. 2001.
[78] M. Di Renzo, D. De Leonardis, F. Graziosi, and F. Santucci, "On the robustness of T_c–DTR UWB receivers to narrow–band interference: Performance analysis and guidelines for system optimization", *IEEE Int. Conf. on Ultra–Wideband*, pp. 77–83, Sep. 2009.

Marco Di Renzo (SM'05–AM'07–M'09) was born in L'Aquila, Italy, in 1978. He received the Laurea (cum laude) and the Ph.D. degrees in Electrical and Information Engineering from the Department of Electrical and Information Engineering, University of L'Aquila, Italy, in April 2003 and January 2007, respectively. From August 2002 to January 2008, he was with the Center of Excellence for Research DEWS, University of L'Aquila, Italy. From February 2008 to April 2009, he was a Research Associate with the Telecommunications Technological Center of Catalonia (CTTC), Barcelona, Spain. From May 2009 to December 2009, he was a Research Fellow with the Institute for Digital Communications (IDCOM), The University of Edinburgh, Edinburgh, United Kingdom (UK).

Since January 2010, he has been a Researcher ("Chargé de Recherche Titulaire") with the French National Center for Scientific Research (CNRS), and a research staff member of the Laboratory of Signals and Systems (L2S), a joint research laboratory of the CNRS, the École Supérieure d'Électricité (SUPÉLEC), and the University of Paris–Sud XI, Paris, France. His main research interests are in the area of wireless communications theory, signal processing, and information theory.

In December 2004, he was a co–founder of WEST Aquila s.r.l. (Wireless Embedded Systems Technologies L'Aquila), an R&D Spin–Off of the Center of Excellence for Research DEWS, where he currently holds the position of Project Manager of two FP7–EU projects. In 2006, he was a Visiting Scholar with the Mobile and Portable Radio Research Group, in the Bradley Dept. of Electrical and Computer Engineering, Virginia Tech, USA.

Dr. Di Renzo was awarded a special mention for the outstanding five–year (1997–2003) academic career from the University of L'Aquila, Italy; a three–year Ph.D. fellowship (ranked 1st) from the Department of Electrical and Information Engineering, University of L'Aquila, Italy, and THALES Communications s.p.a, Chieti, Italy; and a personal "Torres Quevedo" Grant (PTQ–08–01–06437) from the "Ministry of Science and Innovation" in Spain for his research on ultra wide band wireless systems and cooperative localization for wireless sensor networks.

Dr. Di Renzo is a Member of the IEEE and IEEE Communications Society, and serves as reviewer for transactions journals and international conferences. He served as the Publicity Chair of the 2010 International Conference on Mobile Lightweight Wireless Systems. He serves as Technical Program Committee member of many international conferences in communications.

Dario De Leonardis was born in Atri, Italy, in 1984. He received the Bachelor and the Master degrees in Telecommunications Engineering from the Department of Electrical and Information Engineering, University of L'Aquila, Italy, in October 2006 and May 2009, respectively.

From September 2008 to March 2009, he was a Visiting ERASMUS student at the Telecommunications Technological Center of Catalonia (CTTC), Barcelona, Spain, where he conducted research for his Master thesis project on low–complexity receiver design for ultra wide band wireless systems. In April 2010, he received a personal 1–year research grant from the National Inter–University Consortium for Telecommunications (CNIT) to conduct research on "Space Modulation for Multiple–Input–Multiple–Output Wireless Systems", and he was affiliated with the Department of Electrical and Information Engineering and the Center of Excellence for Research DEWS, University of L'Aquila, Italy. Since December 2010, he has been a Ph.D. candidate in the same institution. His main research interests are in the area of wireless communications.

Fabio Graziosi (S'96-M'97) was born in L'Aquila, Italy, in 1968. He received the Laurea degree (cum laude) and the Ph.D. degree in electronic engineering from the University of L'Aquila, L'Aquila, in 1993 and 1997, respectively.

Since February 1997, he has been with the Department of Electrical Engineering, University of L'Aquila, where he is currently an Associate Professor. He is a member of the Executive Committee, Center of Excellence Design methodologies for Embedded controllers, Wireless interconnect and System-on-chip (DEWS), University of L'Aquila, and the Executive Committee, Consorzio Nazionale Interuniversitario per le Telecomunicazioni (CNIT). He is also the Chairman of the Board of Directors of WEST Aquila s.r.l., a spin–off R&D company of the University of L'Aquila and the Center of Excellence DEWS. He is involved in major national and European research programs in the field of wireless systems and he has been a reviewer for major technical journals and international conferences in communications. He also serves as Technical Program Committee (TPC) member and Session Chairman of several international conferences in communications. His current research interests are mainly focused on wireless communication systems with emphasis on wireless sensor networks, ultra wide band communication techniques, cognitive radio and cooperative communications.

Fortunato Santucci (S'93–M'95–SM'00) was born in L'Aquila, Italy, in 1964. He received the Laurea and Ph.D. degrees in electronic engineering from the University of L'Aquila, L'Aquila, in 1989 and 1994, respectively.

In 1989, he was with Selenia Spazio S.p.A., Rome, Italy, where he was engaged in very small aperture terminals (VSAT) networks design. During 1991–1992, he was with the Solid State Electronics Institute (I.E.S.S.), National Research Council (C.N.R.), Rome, where he was involved in the research on superconductor receivers for millimeter wave satellite systems. Since 1994, he has been with the Department of Electrical Engineering, University of L'Aquila, where he is currently an Associate Professor and the Chair of the Program Committee in Telecommunications Engineering. During 1996, he was a Visiting Researcher in the Department of Electrical and Computer Engineering, University of Victoria, Victoria, BC, Canada, where he researched on code division multiple access (CDMA) networks. He is a member of the Executive Committee, Center of Excellence Design Methodologies for Embedded Controllers, Wireless Interconnect and System–on–Chip (DEWS), University of L'Aquila, and the Executive Committee, Consorzio Nazionale Interuniversitario per le Telecomunicazioni (CNIT). He has been a Reviewer for several technical journal in telecommunications, and is currently an Editor of Kluwer Telecommunications Systems. He has participated in various national and European research programs in wireless mobile communications and coordinates research programs funded by industrial partners. His current research interests include communication theory, access control, and radio resource management in wireless systems with special emphasis on technologies for networked embedded systems.

Dr. Santucci is currently an Editor of the IEEE TRANSACTIONS ON COMMUNICATIONS. He is also a member of the technical program committees (TPC) of several conferences in communications. He is a member of the Communications Theory Committee and a Session Chairman of various conferences.